research articles Journal of proteome research

# Proteomic Analysis of IgE-Mediated Secretion by LAD2 Mast Cells

**Matthew C. Gage,[†,‡] Jeffrey N. Keen,[†] Anthony T. Buxton,[†] Maninder K. Bedi,[†] and John B. C. Findlay*[,†]**

*Institute of Membrane and Systems Biology, Faculty of Biological Sciences, LIGHT Laboratories, University of Leeds, Leeds LS2 9JT, United Kingdom, and Division of Cardiovascular and Diabetes Research, Faculty of Medicine and Health, LIGHT Laboratories, University of Leeds, Leeds LS2 9JT, United Kingdom*

**Received February 9, 2009**

The LAD2 cell line is a relatively recent addition to the range of mast cell analogues and is of particular importance as it is the only human analogue which can be stimulated to degranulate in an IgE-dependent manner. Mast cells are tissue-based effector cells which have historically been shown to play an important role in the adaptive immune response, though there is now gathering evidence of their significance as a component of the innate immune system. These functions can be attributed to the ability of mast cells to regulate secretion of a wide variety of potent biologically active mediators through immediate and delayed responses. This well-orchestrated secretory mechanism of the mast cell makes it an ideal model in which to study this event. In this investigation, two-dimensional electrophoresis was employed as part of the proteomic characterization of the LAD2 human mast cell line, focusing in particular on a global analysis of membrane protein relocation after an IgE-mediated stimulatory event. This investigation has identified six membrane-associated protein spots which became phosphorylated upon IgE-mediated activation, 31 protein spots which displayed consistent recruitment to the membrane fraction, and three which were consistently lost from the soluble fraction. The scenario which emerges reveals a series of substantial changes which affect every compartment of the cell, providing evidence for a coordinated response to a secretory stimulus.

**Keywords:** 2-DE • secretion • mast cells • IgE

## Introduction

Mast cells are tissue-based effector cells of the immune system which play a major role in adaptive immunity and also less well-defined roles in innate immunity, inflammation, angiogenesis and tissue remodeling. Mast cells are able to participate in these diverse processes through their ability to regulate secretion of stored potent biologically active mediators.

The key role of the mast cell in adaptive immunity is a consequence of its ability to be primed with allergen-specific IgE through its high-affinity IgE receptor (Fc$\varepsilon$R1).[1] Activation of the mast cell by a multivalent antigen results in both immediate and delayed responses through secretion of preformed mediators from vesicular granules located in their cytoplasm as well as newly synthesized inflammatory mediators and cytokines. These mediators are very effective at promoting a protective response from other effector cells of the immune system. However, the secretory potential of mast cells is also central to the pathophysiology of many allergic diseases. The effects of inappropriate degranulation of mast cells can vary from acute life-threatening episodes of anaphylaxis such as in food allergy, to grass pollen-induced summer rhino conjunctivitis (hay fever) and the chronic ongoing mediator release evident in bronchial asthma.[2]

Allergy-related mast cell diseases stem from inappropriate activation of their rapid or chronic secretory response. This makes the signaling and secretory mechanisms an exciting and rewarding topic to study, particularly from the perspective of therapeutic intervention. Moreover, since the secretory trigger can be reproduced in the laboratory with primary mast cells or specific analogous cell lines and since their subsequent responses are well-orchestrated, mast cells make an excellent model for the study of secretion in general.[3−6]

Because of the lack of an ideal functional human mast cell model, the standard functional mast cell model available has been the Rat Basophilic Leukemia (RBL)-2H3 cell line. However, it was apparent that this did not fully represent normal mast cells in all respects.[7] Thus, the ability to study human mast cells has been limited by the absence of suitable long-term human mast cell cultures. The main human model available to researchers and bearing the closest resemblance to human mast cells has been the human mast cell leukemia cell line (HMC-1). However, HMC-1 cells have two limiting deficiencies: they are growth factor independent, and they inconsistently degranulate to IgE-dependent signals, presumably due to variable expression of the Fc$\varepsilon$R1 $\alpha$-subunit.[8]

* Corresponding author: Professor J. B. C. Findlay, Institute of Membrane and Systems Biology, Faculty of Biological Sciences, LIGHT Laboratories, University of Leeds, Leeds LS2 9JT, United Kingdom.

[†] Institute of Membrane and Systems Biology, Faculty of Biological Sciences.

[‡] Division of Cardiovascular and Diabetes Research, Faculty of Medicine and Health.


10.1021/pr900108w CCC: $40.75 © 2009 American Chemical Society
Published on Web 05/29/2009

In 2003, a report was published on the characterization of a new human mast cell model.[9] The LAD2 cell line was derived from aspirates of bone marrow during the diagnosis of mastocytosis. These cells were established in culture as cell lines and demonstrate stem cell factor dependence and IgE-mediated degranulation. In this study, we have begun a proteomic characterization of the LAD2 cell line's secretory response to IgE-mediated stimulation. By isolating distinct membrane and soluble fractions from activated and control LAD2 cells for analysis using two-dimensional electrophoresis, we have been able to profile a global response of protein relocation events following activation.

## Experimental Procedures

**LAD2 Cell Line Maintenance and Storage.** LAD2 cells for this laboratory were kindly supplied as a live culture by Dr. A. Kirshenbaum (Laboratory of Allergic Diseases, National Institute of Allergy and Infectious Diseases, National Institute of Health, Bethesda, MD 20892-1881). Cells were incubated at 37 °C, 5% $CO_2$ in StemPro-34 serum-free medium (Invitrogen 10639-011), supplemented with 2 mM glutamine, 100 IU/mL penicillin, 50 $\mu$g/mL streptomycin and 100 ng/mL recombinant human stem cell factor. Cells were not allowed to grow above a density of $0.5 \times 10^6$/mL. Hemidepletion was performed weekly allowing expansion of cell numbers. Small amounts of cell aggregates were broken up by gentle pipetting.

**LAD2 Cell Stimulation.** LAD2 cells were centrifuged at 3000 rpm (Hettich, Rotofix 32, swing-out rotor) and resuspended in Tyrode's buffer at $2 \times 10^6$ cells/mL and primed overnight with 500 ng/mL biotinylated human myeloma IgE (US Biological, distributed by Europa Bioproducts Ltd.). Cells were activated the following morning with 500 ng/mL streptavidin and incubated for an appropriate length of time (see specific experiments) and the reaction was stopped by centrifuging the cells at 3000 rpm for 3 min. For inhibition experiments (see Supplementary Figure 1), disodium cromoglycate (DSCG) was dissolved in PBS to the appropriate concentration and added to the cells 2 min prior to cell activation with streptavidin.

***β*-Hexosaminidase Assay.** This assay was carried out in a 96-well plate. To each well, 100 $\mu$L of substrate (100 mM sodium citrate buffer, pH 4.5, 4 mM 4-nitrophenyl-*n*-acetyl-$\beta$-D-glucosamine) was added, followed by 80 $\mu$L of sample to be assayed. The reaction was stopped by the addition of 160 $\mu$L of stop buffer (0.0167 M sodium carbonate, 0.0167 M sodium bicarbonate pH 10). $\beta$-Hexosaminidase release was assessed by measuring samples at 405 nm using a microplate spectrophotometer (Anthos Labtec) and expressed as a percentage of total cellular $\beta$-hexosaminidase.

**Membrane Preparation.** LAD2 cell pellets were resuspended in 4 mL of homogenization buffer (0.25 M sucrose, 1 mM EDTA-$Na_2$, 10 mM HEPES, NaOH to pH 7.4) by gentle pipetting before being homogenized by nitrogen cavitation (exposure to $N_2$ gas at approximately 800 psi for 15 min at 4 °C, followed by forcing through a needle valve). The cell suspension was centrifuged at 3000*g* (5000 rpm) for 10 min using a Sorvall centrifuge with SS34 rotor. The cell lysate was removed and held on ice and the pellet again resuspended in 4 mL of homogenization buffer. These two supernatants were combined and centrifuged at 80 000*g* (50 000 rpm) for 45 min using a Beckman benchtop ultracentrifuge with TLA-100.4 rotor. Aliquots (0.5 mL) of the resulting supernatant were stored at −70 °C; the pellet(s) were resuspended in 1 mL of deionized water and stored in 100 $\mu$L aliquots at −70 °C.

**BCA Protein Assay.** Protein concentrations of extracts were determined in duplicate at 1/2 and 1/10 dilutions (prepared in 1% (w/v) SDS using a microplate version of the BCA assay (Pierce), according to manufacturer's instructions using 1 mg/mL BSA for standard curve, read at 540 nm on a microplate spectrophotometer (Anthos Labtec)).

**2D Electrophoresis (2-DE).** Samples of membrane suspension (100 $\mu$L) were subjected to TCA/acetone precipitation using the PlusOne Clean-up kit (GE Healthcare). Soluble protein samples were first mixed with an equal volume of 24% (w/v) TCA, incubated on ice for a minimum of 1.5 h, centrifuged at 16 000*g* for 5 min and the supernatant was discarded. Processing of protein pellets was continued as for membrane samples using the cleanup kit. Precipitated proteins were allowed to dry in air for up to 5 min and then solubilized in rehydration buffer (7 M urea, 2 M thiourea, 100 mM DTT, 0.5% (v/v) ampholytes, 4% (w/v) CHAPS, 1% (v/v) Triton X-100, trace of bromophenol blue), applied to immobilized pH gradient (IPG) strips (24 cm, pH 4−7, Bio-Rad) and then allowed to equilibrate fully overnight at room temperature. Isoelectric focusing (IEF) was then performed on a Multiphor II system (GE Healthcare) at 3500 V for 70 000 Vh. Following IEF, IPG strips were incubated in equilibration buffer (50 mM Tris-HCl, pH 8.8, 6 M urea, 30% (v/v) glycerol, 2% (w/v) SDS) containing 0.5% (w/v) DTT for 15 min, followed by equilibration buffer containing 4% (w/v) iodoacetamide for 15 min. IPG strips were applied to 10% (w/v) polyacrylamide gels (along with MW markers applied adjacent to the anodic end of the strip) sealed in place using 0.5% (w/v) agarose and subjected to SDS-PAGE in a Protean Plus DoDecaCell electrophoresis tank (Bio-Rad) at a constant 200 V, typically for 5.5 h. Premixed acrylamide (GE Healthcare) was used in accordance with approved health and safety guidelines. Gels were stained with SYPRO Ruby or Pro-Q Diamond (Invitrogen) according to manufacturer's instructions and imaged using an FX Pro Plus fluorimager (Bio-Rad).

**Gel Image Analysis.** Analysis of the gel images was performed using PDQuest 7.1.1 software (Bio-Rad). Parameters for spot detection were set on a "Master" gel (chosen as the most representative from the general experiment) and these parameters were applied to the remaining images in the experiment. The gels were automatically incorporated into a "Matchset" allowing comparison of all gel images. Differences highlighted by the software for each matchset were compared with one another. Spot differences that appeared in all sets (with each of the different analysis methods) were selected for identification after visually confirming the software-identified differences on the original gel images. Differences that appeared in only two of the matchsets were also examined on the third matchset manually to ensure that they had not been overlooked due to a mismatching error and therefore corrected if necessary.

**Protein Spot Excision/Digestion.** Protein spots from the gels were excised either robotically using a ProteomeWorks SpotCutter (Bio-Rad) or manually using a OneTouch Plus spot picker 1.5 mm (Web Scientific Ltd.). Automated trypsin digestion for peptide mass fingerprinting was carried out using a ProteomeWorks MassPREP Station (Waters), including destaining, reduction/alkylation, digestion with trypsin and plate spotting, according to manufacturer's recommended guidelines. For manual processing, gel pieces were washed with 50 mM ammonium bicarbonate/50% (v/v) acetonitrile, dehydrated in acetonitrile, dried, treated with trypsin (20 $\mu$g/mL), mixed with matrix (10 mg/mL $\alpha$-cyano-4-hydroxycinnamic acid

in methanol/acetonitrile (1:1, v/v) mixed with an equal volume of 0.2% (v/v) aqueous TFA) and spotted onto a MALDI plate. For LC-MS/MS, digests were extracted from gel pieces sequentially with water, 5% (v/v) formic acid and 5% (v/v) formic acid/50% (v/v) acetonitrile, combined and vacuum-dried.

**Mass Spectrometry.** Proteins were typically identified using MALDI-MS peptide mass fingerprinting (M@LDI L/R system, Waters). At least 100 laser shots taken in reflectron mode were combined and the spectra processed using Waters MassLynx v4.0 software (background subtracted, smoothed and centroided). Spectra were calibrated both externally using a tryptic digest of alcohol dehydrogenase and internally using a single trypsin autolysis peak ($m/z$ 2211.105 or 1045.564) as a "lockmass" point. Fingerprints were determined manually, eliminating recognized trypsin and keratin peaks prior to selecting monoisotopic masses for interrogation of databases using the WWW-based Mascot database search engine (www.matrixscience.com). Searches were generally performed using the Swiss-Prot database, up to 1 missed cleavage site, mass error of <100 ppm, and variable modifications of carbamidomethyl (C) and oxidation (M). Further details of parameters used and any variations are detailed in Supporting Information. Protein identifications were accepted on the following criteria: (i) more than 4 matching peptides, (ii) a MOWSE score of more than 50, (iii) sequence coverage greater than 10%. Details of peptide mass lists used for searches and proteins identified are supplied in Supporting Information.

Some protein identifications were made using LC-MS/MS, kindly performed by Dr. Jianhe Peng (Cancer Research UK Clinical Centre, St James's University Hospital, Leeds). Analysis of tryptic digests was carried out using an 1100 series nano-LC system (Agilent Technologies) coupled online to a QSTAR XL quadrupole time-of-flight hybrid mass spectrometer (Applied Biosystems). The nano-LC system was configured to use a trap column (5 mm × 0.3 mm, Zorbax 300SB-$C_{18}$, 5 $\mu$m, Agilent Technologies) to desalt and retain tryptic peptides and a microswitch to switch the trap column into the flow path of the nanoanalytical column (150 mm × 75 $\mu$m Zorbax 300SB $C_{18}$, 3 $\mu$m). Mobile phases were 0.1% (v/v) aqueous formic acid (A) and 0.1% (v/v) formic acid in acetonitrile (B). Tryptic peptides were dissolved in 10 $\mu$L of 0.1% (v/v) aqueous TFA and 4 $\mu$L was injected onto the trap column at a flow rate of 20 $\mu$L/min in mobile phase A. After 8 min, the trap column was switched to couple with the analytical column running at 200 nL/min with 10% (v/v) mobile phase B. A 30 min gradient was performed to ramp linearly the concentration of B from 10% to 40% (v/v). The column was washed by ramping to 95% (v/v) B and re-equilibrated at 10% (v/v) B.

The eluate from the nano-LC was directly ionized by spraying through a nanospray emitter (FS360-20-10-D-20, New Objective). Spray voltage was set to 2200 V, with the mass spectrometer operating in a data dependent mode: an MS scan from 400 to 1800 $m/z$ was performed for 1 s; the three most abundant doubly or triply charged ions in the $m/z$ region of 400−1000 and with intensities over 10 counts were selected for MS/MS analysis by collision in a nitrogen gas cell. Each MS/MS analysis was acquired from 80 to 1800 $m/z$ for 1 s in the Enhance All mode and the precursors were then excluded for 200 s.

The MS/MS data were processed using Analyst 2.0 and a script plug in Mascot.dll 1.6b24 (Applied Biosystems), then sent to the local Mascot database search engine (version 2.2.03, Matrix Science) with the following parameters: type of search, MS/MS ion search; instrument type, ESI-Quad-TOF; mass values, monoisotopic; protein mass, unrestricted; precursor mass tolerance, 0.15 Da; fragment ion mass tolerance, 0.1 Da; enzyme, trypsin with 1 missed cleavage site; database, NCBInr (06 May 2009, 8 483 808 sequences); species, human (205 685 sequences); variable protein modifications, carbamidomethyl (C), oxidation (M). A decoy database was used to determine false error rates. Further details are provided in Supporting Information. A minimum of two peptide sequences scoring >36 were required for acceptance of a protein identification.

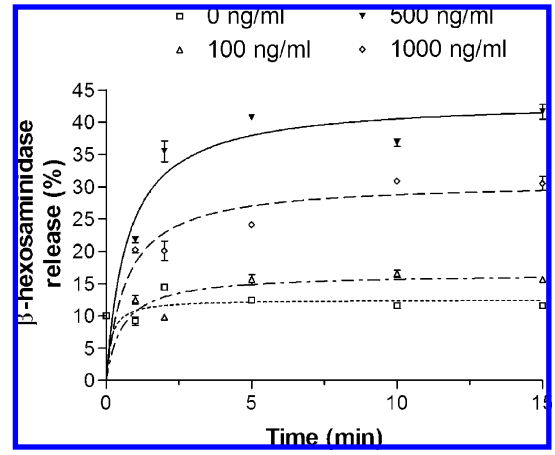


**Figure 1.** Time-course study of IgE-mediated response of LAD2 cells. Three different concentrations of human IgE-biotin conjugate in 1:1 ratio with streptavidin were investigated. Data are presented as means ± SEM, representative of three repeats.

## Results and Discussion

**LAD Cell Stimulation Time Course.** IgE-mediated degranulation of LAD2 cells has been performed previously using human myeloma IgE conjugated to biotin at 100 ng/mL for priming the cells and streptavidin at 100 ng/mL for activation (personal communication from Dr. Yalin Wu of the Laboratory of Allergic Diseases, National Institute of Allergy and Infectious Diseases, National Institute of Health, Bethesda, MD 20892-1881). It was necessary to establish the secretory response over time, addressing particularly the issue of the point at which to arrest the cellular response for protein profiling. Human myeloma IgE-conjugate was used in a 1:1 ratio with streptavidin, as documented previously,[9] and a range of concentrations between 0 and 1000 ng/mL were tested over 15 min. The maximum response occurred at 500 ng/mL (Figure 1).

Degranulation began to plateau by about 5 min after addition of the stimulus. From these experiments, it was decided to use a concentration of 500 ng/mL for both priming and activating the cells, together with cell arrest at 2 min to ensure maximal signal transduction. Like peritoneal mast cells, the secretory response of LAD2 cells was inhibited by DSCG, when added 2 min before the stimulus (see Figure 1 of Supporting Information), demonstrating the biological relevance of using this cell line.

**LAD2 Cell Stimulation Experimental Design.** A membrane and soluble fraction was generated from stimulated and unstimulated cells. These cells were subjected to 2D-electrophoresis in triplicate for comparison. This whole experiment was repeated independently three times, each stimulation giving $\beta$-hexosaminidase release varying between 25 and 40% of total cellular content. The gels were sequentially stained with

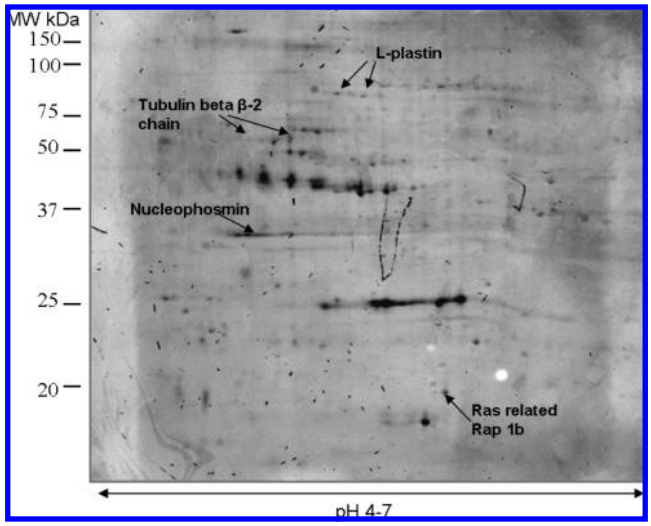


**Figure 2.** Image of representative 2-DE gel of LAD2 membrane fraction stained with Pro-Q Diamond phosphoprotein stain. Six spots showing increased phosphostaining intensity were identified.

**Table 1.** Proteins Showing Increased Phosphorylation upon Stimulation[a]

| protein identified | accession no. | score | peptides matched | sequence coverage (%) | MW (kDa) | p*I* |
|---|---|---|---|---|---|---|
| L-plastin | P13796 | 185 | 17 | 31 | 70.2 | 5.2 |
| L-plastin | P13796 | 105 | 14 | 26 | 70.2 | 5.2 |
| Tubulin $\beta$-2 chain | P07437 | 153 | 15 | 35 | 49.6 | 4.79 |
| Tubulin $\beta$-2 chain | P07437 | 125 | 9 | 25 | 49.6 | 4.79 |
| Nucleophosmin | P06748 | 84 | 6 | 22 | 32.6 | 4.64 |
| Ras-related Rap1b | P61224 | 76 | 7 | 45 | 20.8 | 5.65 |

[a] Identified proteins are shown with their Swiss-Prot accession number, theoretical p*I* and molecular weight. MASCOT search score, number of peptides used for identification, and coverage of each identification are also listed. Score is $-10$ log($p$), where $p$ is the probability that the observed match is a random event. Scores >50 indicate identity or extensive homology at the $p < 0.05$ level.

the Pro-Q Diamond phosphoprotein stain, followed by SYPRO Ruby to detect phosphorylated components and evaluate protein abundance. Up/down regulation of the membrane and soluble fraction for phosphorylation and total protein were subjected to analysis and resulted in three productive data sets. These were detectable increases in phosphostaining of proteins in the membrane fraction upon stimulation, protein recruitment to the membrane upon stimulation, and a loss of protein spots from the soluble supernatant fraction.

**Differences in Membrane Fraction Phosphorylation upon IgE-Mediated Stimulation.** Approximately 150 detected spots from each phosphoprotein-stained gel from each of the three experiments of the membrane fraction from stimulated and control cells were analyzed (18 gels in total). This resulted in 7 spots showing a consistently increased phosphorylation level in the membrane fraction from the stimulated cells. Six of these protein components were identified (Figure 2 and Table 1).

Four different proteins were identified as being phosphorylated upon IgE-mediated stimulation: L-plastin, tubulin $\beta$-2 chain, Rap1b and nucleophosmin, all of which are known to be involved in the secretory process. L-plastin has been shown to become phosphorylated in human neutrophils[10] in response to *N*-formyl-L-methionine-L-leucyl-L-phenylalanine (fMLP). This is particularly relevant because membrane recruitment of

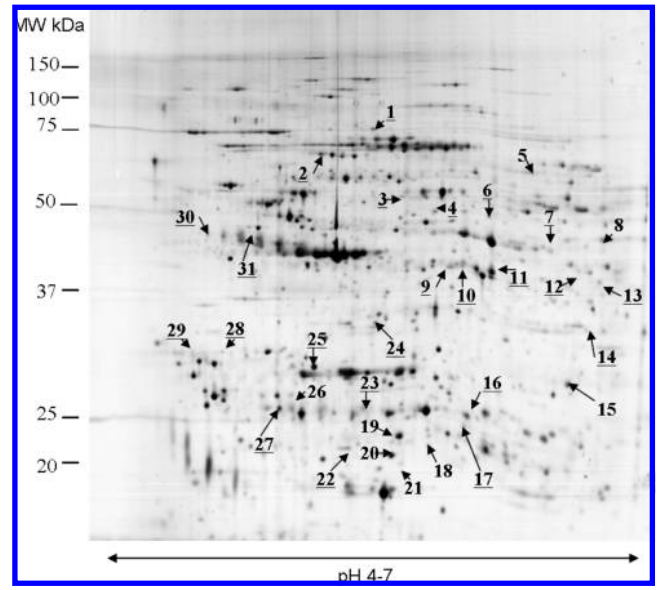


**Figure 3.** Image of representative 2-DE gel of LAD2 membrane fraction stained with SYPRO Ruby, showing protein species recruited to the membrane fraction upon stimulation of cells with IgE. Numbers in bold and underlined indicate spots showing quantitative increase in every gel from all three independent experiments, numbers not in bold but underlined indicate spots showing consistent increase in all but one gel from all three independent experiments.

acylamino-acid-releasing enzyme (implicated in dampening down the immune response[11]) also occurs in response to stimulation (see later). Phosphorylated L-plastin is also involved in the activation of superoxide-generating NADPH oxidase,[12] potentially giving rise to reactive oxygen species (ROS) as a source of intracellular second messengers. A subunit (NDUSF1) of complex 1 of NADPH oxidase is shown in this study to become membrane-associated. In secretion from RBL-2H3 cells,[13] granule motility required the attachment of adjacent microtubules, a process that may be dependent on tubulin. The phosphorylation of tubulin may be necessary for this attachment process. Interestingly, T-plastin interacts with an actin-binding Arp2/3 complex.[14] This investigation reveals Arp3 recruitment to the membrane on stimulation. Rap1b activates the B-Raf kinase and the MEK/ERK cascade. It has also been shown that Rap1b becomes associated with the cytoskeleton in thrombin-activated platelets and may promote assembly of protein complexes. Nucleophosmin is a nuclear protein which has been reported previously to be phosphorylated.[15] A recent report has concluded that nucleophosmin is a nucleus-cytoplasm shuttling protein that is implicated in centrosome duplication, cell cycle progression and stress response.[16] The change observed here suggests an involvement perhaps in the recovery process following cell stimulation.

**Membrane Fraction Abundance Differences.** Changes in spot densities of the membrane fraction were widespread, indicative of the complex mechanisms underpinning the secretory process. Analysis of recruitment and loss of species in the membrane fraction resulted in 31 differences from up to 1000 components which correlated across 18 gels from the three separate experiments (Figure 3).

Spots annotated with a number and underlined are those which showed a quantitative increase in every gel from every experiment analyzed. Spots annotated with a number not

**Table 2.** Proteins Recruited to the Membrane upon Stimulation[a]

| gel position | protein identified | accession no. | score | peptides matched | sequence coverage (%) | MW (kDa) | p*I* |
|---|---|---|---|---|---|---|---|
| 1 | NDUFS1 | P28331 | 90 | 9 | 14 | 79.4 | 5.89 |
| 2 | L-plastin | P13796 | 113 | 11 | 21 | 70.2 | 5.2 |
| 3 | Protein disulfide isomerase A3 | P30101 | 55 | 7 | 11 | 56.7 | 5.98 |
| 4 | Actin-like protein 3 | P61158 | 76 | 7 | 18 | 47.3 | 5.61 |
| 5 | Retinal dehydrogenase | P00352 | 95 | 8 | 21 | 54.7 | 6.29 |
| 6 | Emerin | P50402 | 114 | 9 | 40 | 29 | 5.26 |
| 8 | Septin 11 | Q9NVA2 | 78 | 11 | 26 | 49.2 | 6.38 |
| 10 | Leukocyte elastase inhibitor | P30740 | 93 | 8 | 23 | 42.7 | 5.9 |
| 11 | Leukocyte elastase inhibitor | P30740 | 161 | 15 | 34 | 42.7 | 5.9 |
| 13 | Afadin | P55196 | 72 | 10 | 7 | 205.6 | 6.33 |
| 15 | Purine nucleotide phosphorylase | P00491 | 82 | 9 | 33 | 32.1 | 6.45 |
| 16 | 15-hydroxyprostaglandin dehydrogenase | P15428 | 68 | 6 | 30 | 29 | 5.56 |
| 17 | Growth factor receptor-bound protein 2 | P62993 | 68 | 7 | 27 | 25.2 | 5.89 |
| 18 | Glutathione peroxidase 1 | P07203 | 66 | 5 | 28 | 21.9 | 6.15 |
| 19 | Peroxiredoxin 2 | P32119 | 73 | 7 | 32 | 21.7 | 5.67 |
| 20 | Ras-related protein Rab11b | Q15907 | 77 | 7 | 34 | 24.3 | 5.65 |
| 20 | UMP-CMP kinase | P30085 | 71 | 6 | 35 | 22.2 | 5.44 |
| 20 | Peroxiredoxin 2 | P32119 | 54 | 4 | 23 | 21.7 | 5.67 |
| 21 | Ras-related protein Rap1b | P61224 | 76 | 7 | 45 | 20.8 | 5.65 |
| 22 | Ras-related protein Rab1b | Q9H0U4 | 84 | 6 | 34 | 22.2 | 5.55 |
| 23 | Ras-related protein Rab27b | O00194 | 82 | 9 | 44 | 24.6 | 5.35 |
| 25 | Chloride intracellular channel protein 1 | O00299 | 93 | 9 | 37 | 26.8 | 5.09 |
| 26 | Guanine nucleotide-binding protein subunit alpha-11 | P29992 | 76 | 8 | 23 | 42.1 | 5.51 |
| 27 | Rho-GDP dissociation inhibitor 1 | P52565 | 77 | 6 | 25 | 23.2 | 5.02 |
| 29 | Tropomyosin α4 chain | P67936 | 81 | 9 | 27 | 28.4 | 4.67 |
| 30 | Ribonuclease inhibitor | P13489 | 60 | 6 | 17 | 49.8 | 4.71 |
| 31 | Gamma enolase | P09104 | 115 | 11 | 30 | 47.1 | 4.91 |
| 31 | Golgin subfamily A, member 4 | Q13439 | 72 | 16 | 7 | 25.6 | 5.34 |

[a] Identified proteins are shown with their Swiss-Prot accession number, theoretical p*I* and molecular weight. MASCOT search score, number of peptides used for identification, and coverage of each identification are also listed. Score is $-10 \log(p)$, where $p$ is the probability that the observed match is a random event. Scores >50 indicate identity or extensive homology at the $p < 0.05$ level.

underlined are those which showed an increase in all but one of the gels analyzed. Tables 2 and 3 show the protein identities of the spots highlighted in Figure 3.

**Proteins Recruited to the Membrane Fraction.** The proteins identified can be grouped according to their function (Table 4).

**Signal Transduction.** Afadin is a multidomain protein which may interact with many different partners and complexes leading to the suggestion that it is important in the organization of membrane junctional complexes.[17] Major roles include integrin-mediated cell−cell adhesion and communication through interaction with Rap1 proteins.[18,19] Interestingly, this investigation also reveals the recruitment of Rap1b. The correlated recruitment of Rap1b is crucial for signal transduction. Afadin may also facilitate FcεR1 clustering upon IgE-mediated activation.[20] A picture is emerging, therefore, of a series of interactions at the surface of the membrane which are consistent with the mechanisms for vesicle migration and exocytosis. Rho proteins function as molecular switches, regulating a multitude of biological processes including cell proliferation, apoptosis, differentiation and cytoskeletal reorganization,[21] gene transcription, phagocytosis, vesicular trafficking and regulation of a range of enzymatic functions, for example, NADPH oxidase.[22] Rho GDP dissociation inhibitors (RhoGDI) have been found to extract membrane-bound post-translationally modified GDP-bound proteins from the membrane.[21] Previous reports suggest that stimulated mast cells undergo cytoskeletal rearrangement and vesicular trafficking. Rho GDP dissociation inhibitor 1 identified here may have bound to the membrane to deactivate its complementary GTPase effectors. This result is consistent with previous suggestions that the GDI could move to the membrane to extract GTPases.[21]

Guanine nucleotide-binding protein α-subunit 11 (GNA11) is thought to be activated by proteinase-activated receptors PAR1 and PAR2, two G-protein-coupled receptors present in mast cells.[23] PAR2 agonists (including trypsin and tryptase) induce histamine release through induction of $Ca^{2+}$ mobilization.[23] The up-regulation of GNA11 here is consistent with this action. In human umbilical vein endothelial cells PAR2 activates RhoA, an inhibitor of which (RhoGDI) was shown to be recruited to the membrane fraction in this investigation.[24] Both observations beg the question as to whether the stimulation of secretion involves the signal transduction pathway from PAR2.

Growth factor receptor-bound protein 2 (Grb2) binds directly to several types of activated tyrosine kinase receptors,[25] among which is the FcεR1.[25,26] Grb2 does not possess any membrane-targeting sequences and is therefore most likely to be cytosolic in nonactivated cells. The fact that it becomes associated with the membrane represents a strong proof of principle in this investigation.

**Proteins Involved in Exocytosis.** There are currently more than 60 Rab proteins in the human genome.[27] They are thought to play roles in the specificity of membrane transport steps particularly in long-range vesicular transport within eukaryotic cells.[28] Here, three different Rab proteins were shown to be recruited to the membrane fraction. Rab1b may provide a common link between upstream and downstream components of the vesicular formation machinery, functioning in early compartments of the secretory pathway.[28,29]

**Table 3.** Proteins Recruited to Membrane upon Stimulation, Identified Using LC-MS/MS[a]

| gel position | protein identified | accession no. | score | expect value | peptide sequences | MW (kDa) |
|---|---|---|---|---|---|---|
| 28 | Oxidized protein hydrolase | gil7144648 | 39 | 0.064 | VGFLPSAGK | 81.2 |
| | Acylamino-acid-releasing enzyme | (P13798) | 42 | 0.029 | AESFFQTK | |
| | | | 58 | 0.00055 | VTSVVVDVVPR | |
| | | | 70 | $4.6 \times 10^{-5}$ | ALDVSASDDEIAR | |
| | | | 51 | 0.0029 | TPLLLMLGQEDR + Oxidation (M) | |
| | and Dermcidin | gil16751921 | 47 | 0.0072 | ENAGEDPGLAR | 11.3 |
| | | (P81605) | 41 | 0.035 | DAVEDLESVGK | |
| 24 | Eukaryotic translation elongation | gil4503481 | 38 | 0.076 | QVLEPSFR | 50.1 |
| | factor 1 gamma | (P26641) | 47 | 0.0077 | STFVLDEFK | |
| | | | 93 | $1.9 \times 10^{-7}$ | ALIAAQYSGAQVR | |
| | | | 56 | 0.00082 | LDPGSEETQTLVR | |
| | | | 58 | 0.00055 | KLDPGSEETQTLVR | |
| | and Translation initiation factor | gil496902 | 45 | 0.014 | ELAVQIQK | 46.8 |
| | | (P38919) | 37 | 0.079 | EQIYDVYR | |
| | | | 53 | 0.016 | ETQALILAPTR | |
| | | | 54 | 0.013 | MLVLDEADEMLNK + 2 Oxidation (M) | |
| 9 | L-plastin variant | gil62898171 | 67 | $8.2 \times 10^{-5}$ | IGNFSTDIK | 70.2 |
| | | (Q53FI1) | 50 | 0.0037 | LSPEELLLR | |
| | | | 54 | 0.0017 | QFVTATDVVR | |
| | | | 74 | $1.5 \times 10^{-5}$ | EGESLEDLMK + Oxidation (M) | |
| | | | 59 | 0.00022 | GSVSDEEMMELR + 2 Oxidation (M) | |
| | | | 73 | $1.7 \times 10^{-5}$ | MINLSVPDTIDER + Oxidation (M) | |
| | | | 38 | 0.044 | VYALPEDLVEVNPK | |
| | | | 52 | 0.002 | FSLVGIGGQDLNEGNR | |
| | and Lamin B1 | gil5031877 | 39 | 0.056 | LQIELGK | 66.4 |
| | | (P20700) | 41 | 0.031 | IQELEDLLAK | |
| | | | 61 | 0.0003 | ALYETELADAR | |
| 14 | Unnamed protein product | gil34228 | 45 | 0.017 | LEAALGEAK | 79.3 |
| | (Lamin A/C) | (P02545) | 54 | 0.0017 | SLETENAGLR | |
| | | | 79 | $5.3 \times 10^{-6}$ | ITESEEVVSR | |
| | | | 37 | 0.081 | SGAQASSTPLSPTR | |
| | | | 39 | 0.046 | LQTMKEELDFQK + Oxidation (M) | |
| | and Isopentenyl-diphosphate | gil6225527 | 59 | 0.00043 | NVTLNPDPNEIK | 26.3 |
| | Delta-isomerase 1 | (Q13907) | 54 | 0.0014 | AFSVFLFNTENK | |
| | | | 47 | 0.0073 | KNVTLNPDPNEIK | |
| 12 | Gamma-aminobutyraldehyde | gil1049219 | 37 | 0.085 | EVNLAVQNAK | 53.5 |
| | dehydrogenase (Aldehyde dehydrogenase family 9 member A1) | (P49189) | 78 | $7.1 \times 10^{-6}$ | IGDPLLEDTR | |
| | | | 38 | 0.044 | GIKPVTLELGGK | |
| | | | 54 | 0.0012 | VIATFTCSGEK + Carbamidomethyl (C) | |
| | | | 50 | 0.0038 | VSFTGSVPTGMK + Oxidation (M) | |
| | | | 49 | 0.0049 | VTIEYYSQLK | |
| | and BSCv | gil9836652 | 54 | 0.0014 | LLEYDTVTR | 47.7 |
| | (Adlpocyte plasma membrane-associated protein) | (Q9HDC9) | 37 | 0.069 | LLLSSETPIEGK | |
| 7 | G(M2) activator protein | gil31853 | 54 | 0.0018 | VDLVLEK | 19.3 |
| | (Ganglioside GM2 activator) | (P17900) | 60 | 0.00045 | EGTYSLPK | |
| | | | 53 | 0.0023 | EVAGLWIK | |
| | | | 61 | 0.00035 | IESVLSSSGK | |

[a] Identified proteins are shown with their GenBank accession number, equivalent Swiss-Prot code and theoretical molecular weight. Peptide sequences scoring >36 are shown, with individual peptide scores and expect values. Further information is presented in Supporting Information.

Rab11b is thought to play an essential role in protein recycling from endosomes to the plasma membrane.[30,31] Rab11 proteins are present on secretory vesicles and Rab11b participates in $Ca^{2+}$-regulated exocytosis.[32] Rab27b is expressed in various types of secretory cells that exhibit regulated secretion and may be involved in the maturation and/or secretion of secretory lysosomes.[33]

GAPDH is a glycolytic enzyme which becomes membrane-associated on mast cell activation, confirming a link between GADPH, Rab2, and α-tubulin and membrane fusion.[34] GADPH is also involved in transcriptional regulation,[34] as are several other proteins identified in this investigation (lamin B, lamin A/C and emerin).

Ganglioside GM2 activator is a sphingolipid-binding protein, which extracts GM2 molecules from the membrane.[35] It is expressed in FcεR1-expressing HMC-1 cells[36] and specifically optimises IgE receptor−ligand interactions.[37]

**Table 4.** Groupings of Proteins Recruited to Membrane, Based on Putative Function

| putative function | proteins identified | references |
|---|---|---|
| IgE-mediated signaling | Growth factor receptor-bound protein 2 | 25, 26 |
| Signal transduction | Afadin | 18, 19, 49 |
| | RhoGDP dissociation inhibitor 1 | 21, 22, 50 |
| | Guanine nucleotide-binding protein subunit alpha-11 | 23, 24 |
| | Isopentenyl-diphosphate delta-isomerase 1 | 51 |
| | Retinal dehydrogenase | 52 |
| | Elongation factor 1-$\gamma$ | 53 |
| | Rap1b[a] | 19, 28, 49 |
| Exocytosis | Rab1b | 19, 28, 49 |
| | Rab11b | 30−32 |
| | Rab27b | 33, 54, 55 |
| | Golgin subfamily A member 4 | 56 |
| | Gamma enolase | 57 |
| | Ganglioside GM2 activator | 35 |
| Nuclear involvement | Chloride intracellular channel protein 1 | 38, 39, 58 |
| | Leukocyte elastase inhibitor | 24, 59 |
| | Septin 11 | 40, 41 |
| | Lamin B1 and A/C | 60, 61 |
| | Emerin | 42, 43 |
| | Nucleophosmin[a] | 16 |
| | UMP-CMP kinase | 62, 63 |
| | Purine nucleotide phosphorylase | 64 |
| Redox regulation | Peroxiredoxin 2 | 65 |
| | Glutathione peroxidase 1 | 66 |
| | Protein disulfide isomerase A3 | 67 |
| | NDUFS1 | 68 |
| Cytoskeletal associated | Arp3 | 45 |
| | Tropomyosin α-4 chain | 69 |
| | Tubulin $\beta$-2 chain[a] | 13 |
| | L-plastin[a] | 10, 12, 70 |
| Secreted | Dermcidin | 47, 48 |
| | Acylamino-acid-releasing enzyme | 11 |
| Degradative Enzymes | 15-Hydroxyprostaglandin dehydrogenase | 71, 72 |
| | Ribonuclease inhibitor | 71, 73 |
| | Aldehyde dehydrogenase family 9 member A1 | 74 |

[a] Also shown to become phosphorylated.

**Nuclear Involvement.** Chloride intracellular protein 1 (CLIC1) is one of 7 members of a chloride ion channel family localized to both nucleoplasm and the nuclear membrane.[38] This investigation shows that upon cell stimulation CLIC1 changes to its integral membrane protein form, which supports a suggestion that CLIC1 is implicated in secretory pathways,[39] perhaps by facilitating ion inductances.

Septin 11 is implicated in a variety of processes from cytokinesis to vesicle trafficking specifically at sites where active membrane or cytoplasmic partitioning is occurring.[40] A recent report has linked septin 11 with the exocytosis mechanism in human umbilical vein endothelial cells.[41]

Emerin has been identified previously as an inner nuclear transmembrane protein, associated with the nuclear matrix possibly with lamin. It has been localized to the cytosol as well as to cytoplasmic membranes in cardiomyocytes, HeLa-S3, SaOS-2, MG63 cells and myocardium. There has also been some implication in actin-binding complex formation and signaling[42] and as an anchor for protein complexes in the inner nuclear membrane.[43] In the mast cell, this membrane association clearly occurs and is likely to involve one or more of lamin and cytoskeletal proteins, all potentially involved in vesicle activation and movement.

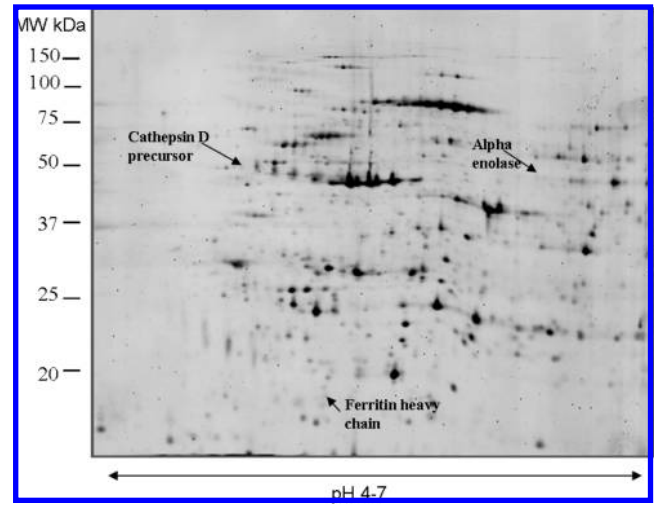


**Figure 4.** Image of representative 2-DE gel of LAD2 soluble fraction stained with SYPRO Ruby, showing locations and identities of protein components lost from the soluble fraction upon IgE-mediated stimulation.

**ROS Production.** Accumulating evidence indicates that, upon stimulation of divergent receptor systems, ROS are intentionally produced and even required for specific biological responses. It has been shown now that stimulation of mast cells through FcεRI induces the production of ROS such as superoxide and $H_2O_2$, possibly by the phagocyte NADPH oxidase homologue.[44] These endogenously produced oxidants have important functions in the regulation of various mast cell responses, including degranulation, leukotriene secretion and cytokine production. The studies reported here indicate that proteins associated with ROS production are recruited to the membrane.

**Cytoskeleton-Associated Proteins.** Actin-like protein 3 (Arp3) interacts with L-plastin and is part of a complex including Arp2 which has a central role in the control of actin polymerization.[45] In relation to secretion, the Arp2/3 complex localizes to the center of the talin ring, close to the point where granules accumulate before secretion. The suggestion is that the Arp2/3 complex can induce motility of endocytic vesicles via the assembly of an actin comet tail which propels the vesicle through the cytoplasm. This raises the interesting possibility that actin polymerization could be a driving force for the propulsion of granules to the plasma membrane.[46] Similarly, the recruitment of tropomyosin α4 chain may also be critical to vesicular movement, reinforcing previous speculations on its role.

**Degradative/Secreted Proteins.** Dermcidin (DCD) was recently discovered as a novel antimicrobial peptide[47] secreted into sweat by mucosal cells of sweat gland coil and is thought to play a key role in innate immunity.[48] Recruitment to the membrane fraction upon mast cell stimulation raises the novel possibility that DCD is secreted from mast cells too.

**Soluble Fraction Abundance Differences.** Analysis of 850−1000 spots in the gels of the soluble fractions revealed 13 components consistently lost from the soluble fraction of stimulated cells. Three of these components were identified successfully (Figure 4 and Table 5).

**Table 5.** Proteins Lost from the Soluble Fraction upon Stimulation[a]

| protein identified | accession no. | score | peptides matched | sequence coverage (%) | MW (kDa) | p*I* |
|---|---|---|---|---|---|---|
| Alpha enolase | P06733 | 96 | 7 | 22 | 47 | 6.99 |
| Ferritin heavy chain | P02794 | 67 | 5 | 25 | 21.1 | 5.3 |
| Cathepsin D precursor | P07339 | 105 | 11 | 31 | 44.5 | 6.1 |

[a] Identified proteins are shown with their Swiss-Prot accession number, theoretical p*I* and molecular weight. MASCOT search score, number of peptides used for identification, and coverage of each identification are also listed. Score is $-10 \log(p)$, where $p$ is the probability that the observed match is a random event. Scores >50 indicate identity or extensive homology at the $p < 0.05$ level.

**Loss of Proteins from the Soluble Fraction upon IgE-Mediated Stimulation.** In general, fewer changes were seen in the soluble fraction, which possesses greater complexity with a wider dynamic range than the membrane fraction. The less-abundant proteins involved in the secretory mechanism constitute only a very limited proportion of this compartment. Moreover, since membrane recruitment usually occurs to only a modest proportion of the cytosolic population, depletion is harder to determine statistically. Thus, experimental evidence so far has shown protein recruitment to membranes. For the secretory mechanism too, the general trend is for protein recruitment to membranes. This is clearly the main observation made in this study.

The adaptor protein Grb2 is an excellent proof of principle for this investigation, being a key facilitator of IgE-mediated signaling in mast cells through its recruitment to the plasma membrane and adaptor properties. This greatly increases the level of confidence that the other proteins identified are relevant to some aspect of the mast cell response. For example, the three Rab proteins identified are heavily involved in vesicular secretion and change from a cytosolic to membrane-bound state when activated. In addition, the cytoskeletal proteins have a broad range of activities which have previously been implicated in secretion. Several of the proteins from the nuclear involvement category have been associated with each other previously and their respective putative roles in transcription also lend themselves to the mast cell response, which would require an assortment of genes to be transcribed and translated for recovery after degranulation. They are also likely to be implicated in complex formation increasingly seen in membrane-associated events.

Certain proteins normally secreted have shown no previous intracellular membrane-binding capacity. That they have been found in the membrane fraction can be explained on the basis of their increased association with vesicles destined for exocytosis. This is a less well-understood area of cellular behavior, but the proteins are consistent with the mast cell response. Dermcidin is an interesting and novel example of this. The two proteins which present the most challenge in relation to the mast cell function are the intracellular chloride channel CLIC1 and emerin. Both have been described as integral membrane proteins and both have shown a soluble cytosolic localization. They would make ideal candidates with which to perform functional proteomics studies and are a good example of how a global approach may uncover unexpected functionality.

## Conclusion

IgE-mediated activation of the LAD2 mast cell line was optimized through stimulant concentration and time-course studies. It was observed that four proteins showed a significant increase in phosphorylation within the membrane fraction. Thirty-one components were recruited to the membrane fraction and 13 spots were depleted from the soluble fraction. Of these consistent changes, 35 different proteins were identified.

Several of the species identified have previously been shown to associate with membranes upon mast cell stimulation, for example, the adaptor protein Grb2. These identifications validated the principle of the approach and are evidence that the system used is one that is highlighting relevant proteins. Some of the identifications were of cytoskeletal proteins such as tubulin and tropomyosin, whose association with a membrane is a prerequisite of vesicle migration and fusion and so are completely appropriate.

Proteins which have not been implicated previously in mast cell secretion have also been identified, such as Rap1b and GNA11, whose activities are known and which are logical candidates to participate in the mast cell secretion process, and ones such as enolase which are now displaying new and additional functionalities. As the technologies used here become more robust and sensitive, a more complete picture of the mast cell secretory response will emerge.

**Abbreviations:** ROS, reactive oxygen species.

**Acknowledgment.** We would like to thank Dr. A. Kirshenbaum and Dr. Yalin Wu for generously supplying the initial LAD2 cells and technical advice. We would also like to thank Dr. Jianhe Peng for LC-MS/MS protein identifications. Work was funded by BBSRC in the form of a studentship awarded to M.C.G.

**Supporting Information Available:** Inhibition of LAD2 cells by disodium cromoglycate; control gel image of representative 2-DE gel of LAD2 membrane fraction stained with Pro-Q Diamond phosphoprotein stain; control gel image of representative 2-DE gel of LAD2 membrane fraction stained with SYPRO Ruby, after stimulation of cells with IgE; MALDI peak list data; tables of proteins showing increased phosphorylation upon stimulation; proteins recruited to the membrane upon stimulation; proteins lost from the soluble fraction upon stimulation. This material is available free of charge via the Internet at http://pubs.acs.org.

## References

(1) Peachell, P. Targeting the mast cell in asthma. *Curr. Opin. Pharmacol.* **2005**, *5*, 251–256.
(2) Bradding, P. C3a, mast cells, and asthma. *FASEB J.* **2005**, *19*, 1585.
(3) Quesada, I.; Chin, W. C.; Steed, J.; Campos-Bedolla, P.; Verdugo, P. Mouse mast cell secretory granules can function as intracellular ionic oscillators. *Biophys. J.* **2001**, *80*, 2133–2139.
(4) Breckenridge, L. J.; Almers, W. Final steps in exocytosis observed in a cell with giant secretory granules. *Proc. Natl. Acad. Sci. U.S.A.* **1987**, *84*, 1945–1949.
(5) Marszalek, P. E.; Farrell, B.; Verdugo, P.; Fernandez, J. M. Kinetics of release of serotonin from isolated secretory granules. I. Amperometric detection of serotonin from electroporated granules. *Biophys. J.* **1997**, *73*, 1160–1168.
(6) Monck, J. R.; Oberhauser, A. F.; Keating, T. J.; Fernandez, J. M. Thin-section ratiometric Ca2+ images obtained by optical sectioning of fura-2 loaded mast cells. *J. Cell Biol.* **1992**, *116*, 745–759.
(7) Carroll, K. M.; Carey, E. M.; Helm, B. A. Protein mapping in rat basophilic leukaemia cells. *J. Chromatogr., B: Anal. Technol. Biomed. Life Sci.* **2002**, *771*, 289–301.
(8) Nilsson, G.; Blom, T.; Kusche-Gullberg, M.; Kjellen, L.; Butterfield, J. H.; Sundstrom, C.; Nilsson, K.; Hellman, L. Phenotypic characterization of the human mast-cell line HMC-1. Scand. *J. Immunol.* **1994**, *39*, 489–498.
(9) Kirshenbaum, A. S.; Akin, C.; Wu, Y.; Rottem, M.; Goff, J. P.; Beaven, M. A.; Rao, V. K.; Metcalfe, D. D. Characterization of novel stem

cell factor responsive human mast cell lines LAD 1 and 2 established from a patient with mast cell sarcoma/leukemia; activation following aggregation of FcepsilonRI or FcgammaRI. *Leuk. Res.* **2003**, *27*, 677–682.
(10) Paclet, M. H.; Davis, C.; Kotsonis, P.; Godovac-Zimmermann, J.; Segal, A. W.; Dekker, L. V. N-Formyl peptide receptor subtypes in human neutrophils activate L-plastin phosphorylation through different signal transduction intermediates. *Biochem. J.* **2004**, *377*, 469–477.
(11) Perrier, J.; Durand, A.; Giardina, T.; Puigserver, A. Catabolism of intracellular N-terminal acetylated proteins: involvement of acylpeptide hydrolase and acylase. *Biochimie* **2005**, *87*, 673–685.
(12) Oshizawa, T.; Yamaguchi, T.; Suzuki, K.; Yamamoto, Y.; Hayakawa, T. Possible involvement of optimally phosphorylated L-plastin in activation of superoxide-generating NADPH oxidase. *J. Biochem.* **2003**, *134*, 827–834.
(13) Smith, A. J.; Pfeiffer, J. R.; Zhang, J.; Martinez, A. M.; Griffiths, G. M.; Wilson, B. S. Microtubule-dependent transport of secretory vesicles in RBL-2H3 cells. *Traffic* **2003**, *4*, 302–312.
(14) Giganti, A.; Plastino, J.; Janji, B.; Van Troys, M.; Lentz, D.; Ampe, C.; Sykes, C.; Friederich, E. Actin-filament cross-linking protein T-plastin increases Arp2/3-mediated actin-based movement. *J. Cell Sci.* **2005**, *118*, 1255–1265.
(15) Chan, P. K.; Liu, Q. R.; Durban, E. The major phosphorylation site of nucleophosmin (B23) is phosphorylated by a nuclear kinase II. *Biochem. J.* **1990**, *270*, 549–552.
(16) Mariano, A. R.; Colombo, E.; Luzi, L.; Martinelli, P.; Volorio, S.; Bernard, L.; Meani, N.; Bergomas, R.; Alcalay, M.; Pelicci, P. G. Cytoplasmic localization of NPM in myeloid leukemias is dictated by gain-of-function mutations that create a functional nuclear export signal. *Oncogene* **2006**, *25*, 4376–4380.
(17) Ikeda, W.; Nakanishi, H.; Miyoshi, J.; Mandai, K.; Ishizaki, H.; Tanaka, M.; Togawa, A.; Takahashi, K.; Nishioka, H.; Yoshida, H.; Mizoguchi, A.; Nishikawa, S.; Takai, Y. Afadin: A key molecule essential for structural organization of cell-cell junctions of polarized epithelia during embryogenesis. *J. Cell Biol.* **1999**, *146*, 1117–1132.
(18) Miyoshi, J.; Takai, Y. Molecular perspective on tight-junction assembly and epithelial polarity. *Adv. Drug Delivery Rev.* **2005**, *57*, 815–855.
(19) Takai, Y.; Nakanishi, H. Nectin and afadin: novel organizers of intercellular junctions. *J. Cell Sci.* **2003**, *116*, 17–27.
(20) Wilson, B. S.; Pfeiffer, J. R.; Oliver, J. M. Observing FcepsilonRI signaling from the inside of the mast cell membrane. *J. Cell Biol.* **2000**, *149*, 1131–1142.
(21) Olofsson, B. Rho guanine dissociation inhibitors: pivotal molecules in cellular signalling. *Cell Signalling* **1999**, *11*, 545–554.
(22) Dovas, A.; Couchman, J. R. RhoGDI: multiple functions in the regulation of Rho family GTPase activities. *Biochem. J.* **2005**, *390*, 1–9.
(23) Moormann, C.; Artuc, M.; Pohl, E.; Varga, G.; Buddenkotte, J.; Vergnolle, N.; Brehler, R.; Henz, B. M.; Schneider, S. W.; Luger, T. A.; Steinhoff, M. Functional characterization and expression analysis of the proteinase-activated receptor-2 in human cutaneous mast cells. *J. Invest. Dermatol.* **2006**, *126*, 746–755.
(24) Steinhoff, M.; Buddenkotte, J.; Shpacovitch, V.; Rattenholl, A.; Moormann, C.; Vergnolle, N.; Luger, T. A.; Hollenberg, M. D. Proteinase-activated receptors: transducers of proteinase-mediated signaling in inflammation and immune response. *Endocr. Rev.* **2005**, *26*, 1–43.
(25) Buday, L. Membrane-targeting of signalling molecules by SH2/SH3 domain-containing adaptor proteins. *Biochim. Biophys. Acta, 1422* **1999**, 187–204.
(26) Turner, H.; Reif, K.; Rivera, J.; Cantrell, D. A. Regulation of the adapter molecule Grb2 by the Fc epsilon R1 in the mast cell line RBL2H3. *J. Biol. Chem.* **1995**, *270*, 9500–9506.
(27) Hammer, J. A., III.; Wu, X. S. Rabs grab motors: defining the connections between Rab GTPases and motor proteins. *Curr. Opin. Cell Biol.* **2002**, *14*, 69–75.
(28) Plutner, H.; Cox, A. D.; Pind, S.; Khosravi-Far, R.; Bourne, J. R.; Schwaninger, R.; Der, C. J.; Balch, W. E. Rab1b regulates vesicular transport between the endoplasmic reticulum and successive Golgi compartments. *J. Cell Biol.* **1991**, *115*, 31–43.
(29) Tisdale, E. J.; Bourne, J. R.; Khosravi-Far, R.; Der, C. J.; Balch, W. E. GTP-binding mutants of rab1 and rab2 are potent inhibitors of vesicular transport from the endoplasmic reticulum to the Golgi complex. *J. Cell Biol.* **1992**, *119*, 749–761.
(30) Junutula, J. R.; Schonteich, E.; Wilson, G. M.; Peden, A. A.; Scheller, R. H.; Prekeris, R. Molecular characterization of Rab11 interactions with members of the family of Rab11-interacting proteins. *J. Biol. Chem.* **2004**, *279*, 33430–33437.
(31) Scapin, S. M.; Carneiro, F. R.; Alves, A. C.; Medrano, F. J.; Guimaraes, B. G.; Zanchin, N. I. The crystal structure of the small GTPase Rab11b reveals critical differences relative to the Rab11a isoform. *J. Struct. Biol.* **2006**, *154*, 260–268.
(32) Khvotchev, M. V.; Ren, M.; Takamori, S.; Jahn, R.; Sudhof, T. C. Divergent functions of neuronal Rab11b in Ca2+-regulated versus constitutive exocytosis. *J. Neurosci.* **2003**, *23*, 10531–10539.
(33) Fukuda, M. Versatile role of Rab27 in membrane trafficking: focus on the Rab27 effector families. *J. Biochem.* **2005**, *137*, 9–16.
(34) Glaser, P. E.; Han, X.; Gross, R. W. Tubulin is the endogenous inhibitor of the glyceraldehyde 3-phosphate dehydrogenase isoform that catalyzes membrane fusion: Implications for the coordinated regulation of glycolysis and membrane fusion. *Proc. Natl. Acad. Sci. U.S.A.* **2002**, *99*, 14104–14109.
(35) Mundel, T. M.; Heid, H. W.; Mahuran, D. J.; Kriz, W.; Mundel, P. Ganglioside GM2-activator protein and vesicular transport in collecting duct intercalated cells. *J. Am. Soc. Nephrol.* **1999**, *10*, 435–443.
(36) Zuberbier, T.; Guhl, S.; Hantke, T.; Hantke, C.; Welker, P.; Grabbe, J.; Henz, B. M. Alterations in ganglioside expression during the differentiation of human mast cells. *Exp. Dermatol.* **1999**, *8*, 380–387.
(37) Zuberbier, T.; Pfrommer, C.; Beinholzl, J.; Hartmann, K.; Ricklinkat, J.; Czarnetzki, B. M. Gangliosides enhance IgE receptor-dependent histamine and LTC4 release from human mast cells. *Biochim. Biophys. Acta* **1995**, *1269*, 79–84.
(38) Valenzuela, S. M.; Martin, D. K.; Por, S. B.; Robbins, J. M.; Warton, K.; Bootcov, M. R.; Schofield, P. R.; Campbell, T. J.; Breit, S. N. Molecular cloning and expression of a chloride ion channel of cell nuclei. *J. Biol. Chem.* **1997**, *272*, 12575–12582.
(39) Jentsch, T. J.; Stein, V.; Weinreich, F.; Zdebik, A. A. Molecular structure and physiological function of chloride channels. *Physiol. Rev.* **2002**, *82*, 503–568.
(40) Martinez, C.; Ware, J. Mammalian septin function in hemostasis and beyond. *Exp. Biol. Med.* **2004**, *229*, 1111–1119.
(41) Blaser, S.; Roseler, S.; Rempp, H.; Bartsch, I.; Bauer, H.; Lieber, M.; Lessmann, E.; Weingarten, L.; Busse, A.; Huber, M.; Zieger, B. Human endothelial cell septins: SEPT11 is an interaction partner of SEPT5. *J. Pathol.* **2006**, *210*, 103–110.
(42) Manta, P.; Terzis, G.; Papadimitriou, C.; Kontou, C.; Vassilopoulos, D. Emerin expression in tubular aggregates. *Acta Neuropathol.* **2004**, *107*, 546–552.
(43) Bengtsson, L.; Wilson, K. L. Multiple and surprising new functions for emerin, a nuclear membrane protein. *Curr. Opin. Cell Biol.* **2004**, *16*, 73–79.
(44) Suzuki, Y.; Yoshimaru, T.; Inoue, T.; Niide, O.; Ra, C. Role of oxidants in mast cell activation. *Chem. Immunol. Allergy* **2005**, *87*, 32–42.
(45) Machesky, L. M.; Gould, K. L. The Arp2/3 complex: a multifunctional actin organizer. *Curr. Opin. Cell Biol.* **1999**, *11*, 117–121.
(46) Stinchcombe, J. C.; Barral, D. C.; Mules, E. H.; Booth, S.; Hume, A. N.; Machesky, L. M.; Seabra, M. C.; Griffiths, G. M. Rab27a is required for regulated secretion in cytotoxic T lymphocytes. *J. Cell Biol.* **2001**, *152*, 825–834.
(47) Schittek, B.; Hipfel, R.; Sauer, B.; Bauer, J.; Kalbacher, H.; Stevanovic, S.; Schirle, M.; Schroeder, K.; Blin, N.; Meier, F.; Rassner, G.; Garbe, C. Dermcidin: a novel human antibiotic peptide secreted by sweat glands. *Nat. Immunol.* **2001**, *2*, 1133–1137.
(48) Rieg, S.; Seeber, S.; Steffen, H.; Humeny, A.; Kalbacher, H.; Stevanovic, S.; Kimura, A.; Garbe, C.; Schittek, B. Generation of multiple stable dermcidin-derived antimicrobial peptides in sweat of different body sites. *J. Invest. Dermatol.* **2006**, *126*, 354–365.
(49) Xie, Z.; Huganir, R. L.; Penzes, P. Activity-dependent dendritic spine structural plasticity is regulated by small GTPase Rap1 and its target AF-6. *Neuron, 48* **2005**, 605–618.
(50) Bishop, A. L.; Hall, A. Rho GTPases and their effector proteins. *Biochem. J.* **2000**, *348 Pt 2*, 241–255.
(51) Chen, H. T.; Mehan, R. S.; Gupta, S. D.; Goldberg, I.; Shechter, I. Involvement of farnesyl protein transferase (FPTase) in FcarepsilonRI-induced activation of RBL-2H3 mast cells. *Arch. Biochem. Biophys.* **1999**, *364*, 203–208.
(52) Hirasawa, N.; Kagechika, H.; Shudo, K.; Ohuchi, K. Inhibition by retinoids of antigen-induced IL-4 production in rat mast cell line RBL-2H3. *Life Sci.* **2001**, *68*, 1287–1294.
(53) Cho, D. I.; Oak, M. H.; Yang, H. J.; Choi, H. K.; Janssen, G. M.; Kim, K. M. Direct and biochemical interaction between dopamine D3 receptor and elongation factor-1Bbetagamma. *Life Sci.* **2003**, *73*, 2991–3004.

(54) Chen, X.; Li, C.; Izumi, T.; Ernst, S. A.; Andrews, P. C.; Williams, J. A. Rab27b localizes to zymogen granules and regulates pancreatic acinar exocytosis. *Biochem. Biophys. Res. Commun.* **2004**, *323*, 1157–1162.
(55) Izumi, T.; Gomi, H.; Kasai, K.; Mizutani, S.; Torii, S. The roles of Rab27 and its effectors in the regulated secretory pathways. *Cell Struct. Funct.* **2003**, *28*, 465–474.
(56) Derby, M. C.; van Vliet, C.; Brown, D.; Luke, M. R.; Lu, L.; Hong, W.; Stow, J. L.; Gleeson, P. A. Mammalian GRIP domain proteins differ in their membrane binding properties and are recruited to distinct domains of the TGN. *J. Cell Sci.* **2004**, *117*, 5865–5874.
(57) Ueta, H.; Nagasawa, H.; Oyabu-Manabe, Y.; Toida, K.; Ishimura, K.; Hori, H. Localization of enolase in synaptic plasma membrane as an alphagamma heterodimer in rat brain. *Neurosci. Res.* **2004**, *48*, 379–386.
(58) Littler, D. R.; Harrop, S. J.; Fairlie, W. D.; Brown, L. J.; Pankhurst, G. J.; Pankhurst, S.; DeMaere, M. Z.; Campbell, T. J.; Bauskin, A. R.; Tonini, R.; Mazzanti, M.; Breit, S. N.; Curmi, P. M. The intracellular chloride ion channel protein CLIC1 undergoes a redox-controlled structural transition. *J. Biol. Chem.* **2004**, *279*, 9298–9305.
(59) Belmokhtar, C. A.; Torriglia, A.; Counis, M. F.; Courtois, Y.; Jacquemin-Sablon, A.; Segal-Bendirdjian, E. Nuclear translocation of a leukocyte elastase Inhibitor/Elastase complex during staurosporine-induced apoptosis: role in the generation of nuclear L-DNase II activity. *Exp. Cell Res.* **2000**, *254*, 99–109.
(60) Hutchison, C. J.; Worman, H. J. A-type lamins: guardians of the soma. *Nat. Cell Biol.* **2004**, *6*, 1062–1067.
(61) Moisan, E.; Girard, D. Cell surface expression of intermediate filament proteins vimentin and lamin B1 in human neutrophil spontaneous apoptosis. *J. Leukocyte Biol.* **2006**, *79*, 489–498.
(62) Liou, J. Y.; Dutschman, G. E.; Lam, W.; Jiang, Z.; Cheng, Y. C. Characterization of human UMP/CMP kinase and its phosphorylation of D- and L-form deoxycytidine analogue monophosphates. *Cancer Res.* **2002**, *62*, 1624–1631.
(63) Van Rompay, A. R.; Johansson, M.; Karlsson, A. Phosphorylation of deoxycytidine analog monophosphates by UMP-CMP kinase: molecular characterization of the human enzyme. *Mol. Pharmacol.* **1999**, *56*, 562–569.
(64) Canduri, F.; Silva, R. G.; dos Santos, D. M.; Palma, M. S.; Basso, L. A.; Santos, D. S.; de, A. W., Jr. Structure of human PNP complexed with ligands. *Acta Crystallogr., D: Biol. Crystallogr.* **2005**, *61*, 856–862.
(65) Chang, J. W.; Lee, S. H.; Lu, Y.; Yoo, Y. J. Transforming growth factor-beta1 induces the non-classical secretion of peroxiredoxin-I in A549 cells. *Biochem. Biophys. Res. Commun.* **2006**, *345*, 118–123.
(66) Kato, S.; Saeki, Y.; Aoki, M.; Nagai, M.; Ishigaki, A.; Itoyama, Y.; Kato, M.; Asayama, K.; Awaya, A.; Hirano, A.; Ohama, E. Histological evidence of redox system breakdown caused by superoxide dismutase 1 (SOD1) aggregation is common to SOD1-mutated motor neurons in humans and animal models. *Acta Neuropathol.* **2004**, *107*, 149–158.
(67) Janiszewski, M.; Lopes, L. R.; Carmo, A. O.; Pedro, M. A.; Brandes, R. P.; Santos, C. X.; Laurindo, F. R. Regulation of NAD(P)H oxidase by associated protein disulfide isomerase in vascular smooth muscle cells. *J. Biol. Chem.* **2005**, *280*, 40813–40819.
(68) Ricci, J. E.; Munoz-Pinedo, C.; Fitzgerald, P.; Bailly-Maitre, B.; Perkins, G. A.; Yadava, N.; Scheffler, I. E.; Ellisman, M. H.; Green, D. R. Disruption of mitochondrial function during apoptosis is mediated by caspase cleavage of the p75 subunit of complex I of the electron transport chain. *Cell* **2004**, *117*, 773–786.
(69) Helfman, D. M.; Berthier, C.; Grossman, J.; Leu, M.; Ehler, E.; Perriard, E.; Perriard, J. C. Nonmuscle tropomyosin-4 requires coexpression with other low molecular weight isoforms for binding to thin filaments in cardiomyocytes. *J. Cell Sci.* **1999**, *112* (Pt. 3), 371–380.
(70) Jones, S. L.; Brown, E. J. FcgammaRII-mediated adhesion and phagocytosis induce L-plastin phosphorylation in human neutrophils. *J. Biol. Chem.* **1996**, *271*, 14623–14630.
(71) Moenner, M.; Vosoghi, M.; Ryazantsev, S.; Glitz, D. G. Ribonuclease inhibitor protein of human erythrocytes: characterization, loss of activity in response to oxidative stress, and association with Heinz bodies. *Blood Cells Mol. Dis.* **1998**, *24*, 149–164.
(72) Nomura, T.; Lu, R.; Pucci, M. L.; Schuster, V. L. The two-step model of prostaglandin signal termination: in vitro reconstitution with the prostaglandin transporter and prostaglandin 15 dehydrogenase. *Mol. Pharmacol.* **2004**, *65*, 973–978.
(73) Teufel, D. P.; Kao, R. Y.; Acharya, K. R.; Shapiro, R. Mutational analysis of the complex of human RNase inhibitor and human eosinophil-derived neurotoxin (RNase 2). *Biochemistry* **2003**, *42*, 1451–1459.
(74) Zimatkin, S. M.; Anichtchik, O. V. Alcohol-histamine interactions. *Alcohol Alcohol.* **1999**, *34*, 141–147.

PR900108W

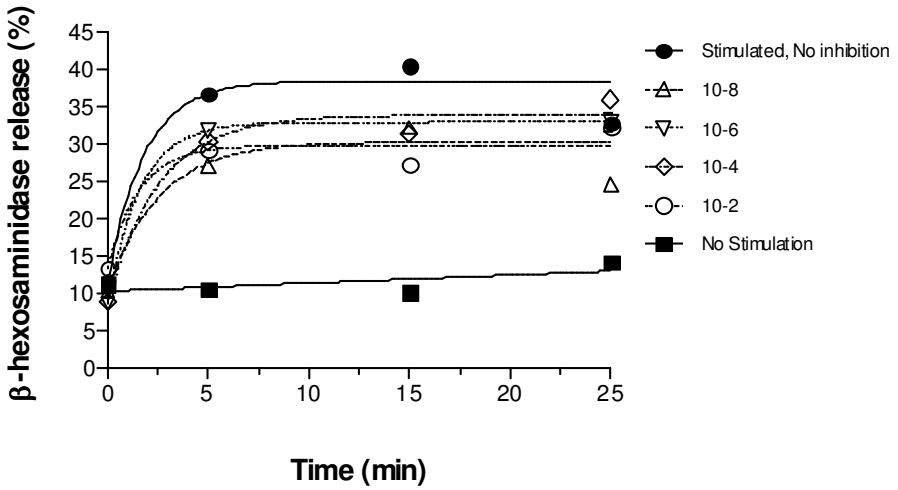


Figure 1: Inhibition of LAD2 cells by disodium cromoglycate. Four different concentrations of DSCG were investigated, with application to cells 2 minutes before activation. Cells were activated with human IgE-biotin conjugate/streptavidin (in 1:1 ratio) at 500 ng/ml.

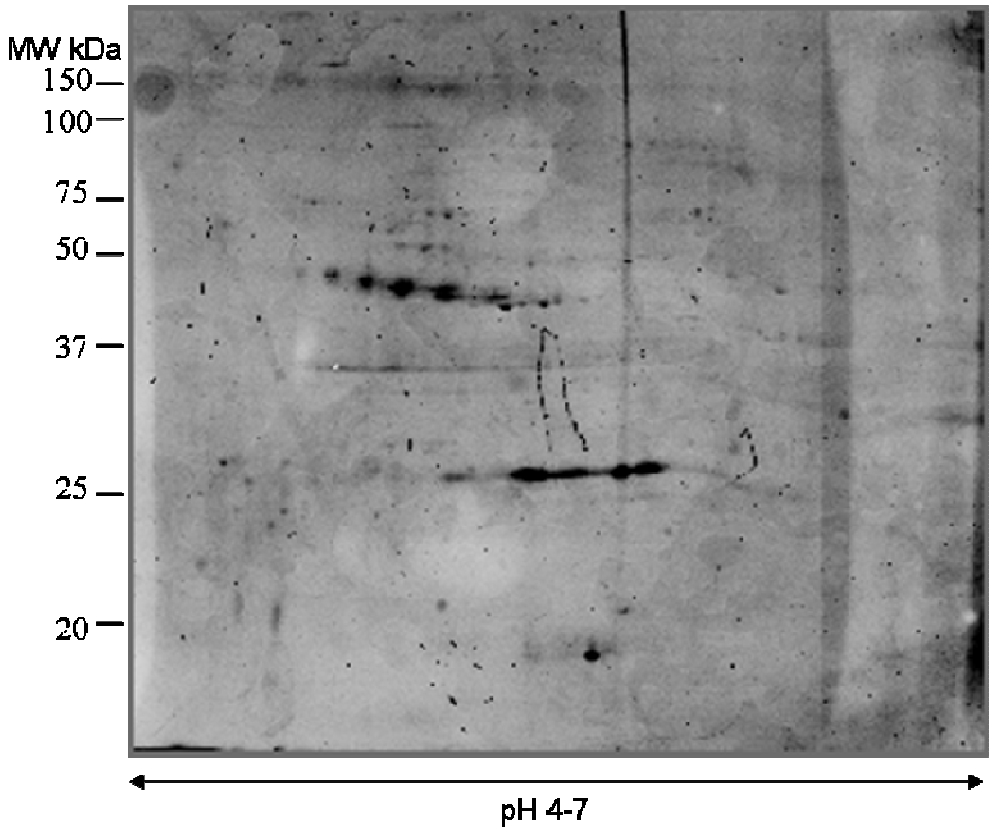


Figure 2: Control gel image of representative 2-DE gel of LAD2 membrane fraction stained with Pro-Q® Diamond phosphoprotein stain.

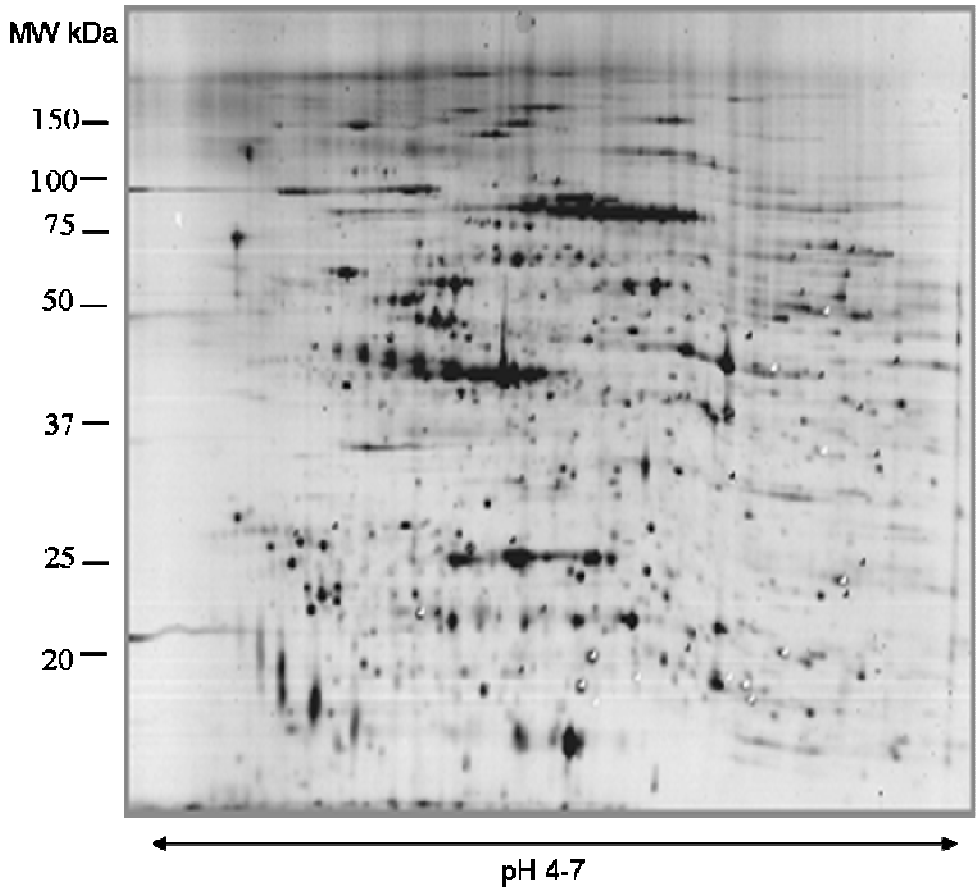


Figure 3: Control gel image of representative 2-DE gel of LAD2 membrane fraction stained with SYPRO® Ruby, after stimulation of cells with IgE.

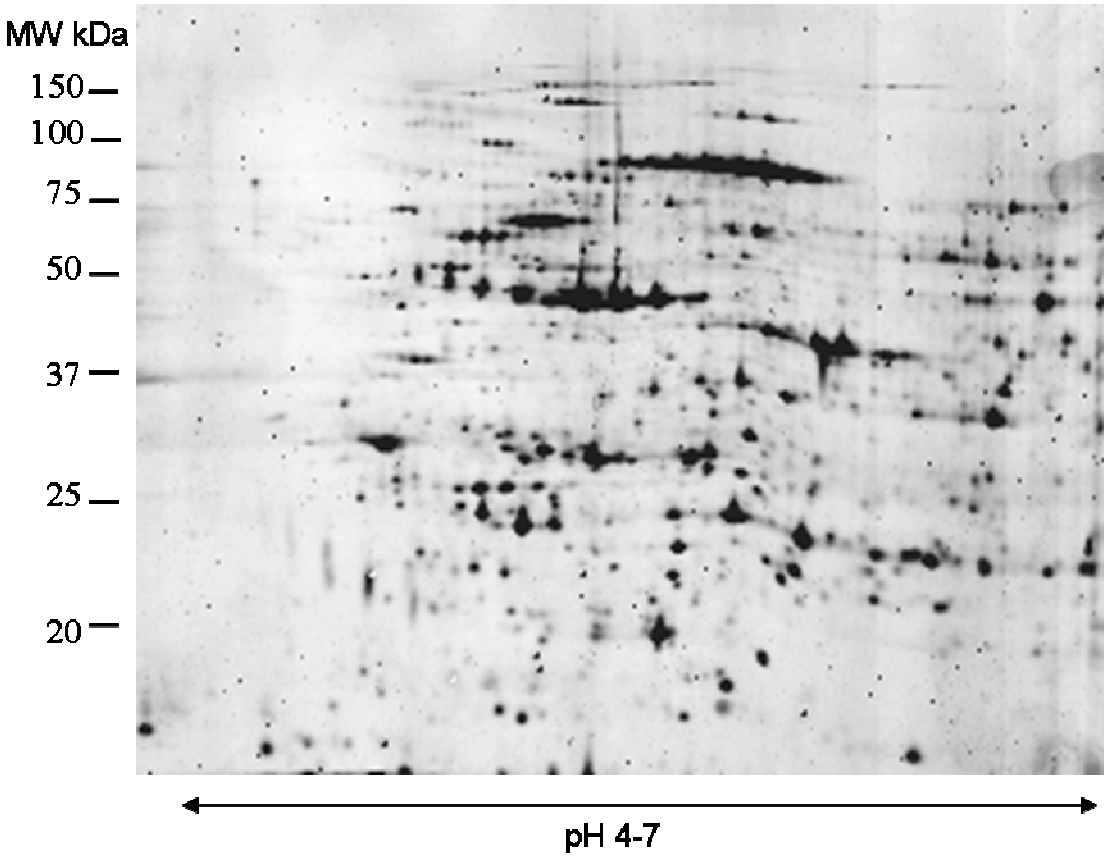


Figure 4: Control gel image of representative 2-DE gel of LAD2 soluble fraction stained with SYPRO® Ruby, after stimulation of cells with IgE.

**MALDI Peak List Data**

Spectra were collected and processed as described in Methods section of paper. Frequently-observed trypsin and keratin peaks were excluded in the generation of peak lists of monoisotopic ions. Peaks lists were used to search the SwissProt database using the Mascot search engine (www.matrixscience.com). The data presented below provide details of peak masses, search parameters and proteins identified.

**Table 1: Proteins showing increased phosphorylation upon stimulation.**

Peptide mass lists are tabulated below, along with Mascot search summary for each protein spot.

MALDI plate and spot number
SwissProt accession number, SwissProt code, protein name
[MOWSE score, expect value, matching peptides/total peptides, percentage coverage; theoretical MW, pI]
Scores in red indicate a statistically significant identification ($p<0.05$) from Mascot search.

**Plate 88**

Gel stain: ProQ Diamond phosphostain and SYPRO Ruby protein stain
Database: SwissProt 48.6 (259907 sequences) – 16 Dec 2005
Taxonomy: unrestricted
Error tolerance: 50 ppm
Variable modifications: CAM-C, Met-ox, prop-C

Any deviations from these parameters are indicated adjacent to spot number.

**88-G7**
**P13796 (PLSL_HUMAN) L-plastin**
**[185 8.2e-14 17/23 31%; 70.2K 5.20]**

| | | | | | |
|---|---|---|---|---|---|
| 917.384 | 942.524 | 994.513 | 998.516 | 1012.589 | 1069.592 |
| 1117.565 | 1118.570 | 1135.586 | 1154.572 | 1186.589 | 1303.627 |
| 1319.612 | 1335.616 | 1431.752 | 1459.655 | 1518.727 | 1534.741 |
| 1537.765 | 1585.828 | 1675.822 | 1759.847 | 1893.850 | |

**88-H7**
**P13796 (PLSL_HUMAN) L-plastin**
**[105 8.2e-06 14/33 26%; 70.2K 5.20]**

| | | | | | |
|---|---|---|---|---|---|
| 908.960 | 942.547 | 945.556 | 976.470 | 994.536 | 998.525 |
| 1069.624 | 1082.052 | 1098.027 | 1117.576 | 1118.579 | 1132.529 |
| 1135.609 | 1186.550 | 1251.542 | 1303.611 | 1319.618 | 1335.599 |
| 1365.650 | 1414.560 | 1490.630 | 1499.675 | 1516.686 | 1518.736 |
| 1585.826 | 1675.826 | 1700.743 | 1759.849 | 1775.826 | 1790.863 |
| 1875.801 | 1893.845 | 1954.050 | | | |

**88-D7 (Taxonomy: human)**
**P07437 (TBB2C_HUMAN) Tubulin beta-2C chain**
**[153 2.8e-11 15/29 35%; 49.8K 4.79]**

| | | | | | |
|---|---|---|---|---|---|
| 1028.526 | 1039.593 | 1063.519 | 1069.603 | 1077.541 | 1130.595 |
| 1159.635 | 1175.620 | 1245.602 | 1261.595 | 1287.730 | 1301.650 |
| 1328.662 | 1335.715 | 1397.686 | 1401.690 | 1406.688 | 1435.766 |
| 1462.713 | 1617.821 | 1631.846 | 1647.832 | 1659.901 | 1701.916 |
| 1707.868 | 1718.895 | 1728.845 | 1873.929 | 1959.001 | |

**88-E7 (Taxonomy: human; error tolerance: 100 ppm)**
**P07437 (TBB2_HUMAN) Tubulin beta-2 chain**
**[125 1.8e-08 9/10 25%; 49.6K 4.78]**

| | | | | | |
|---|---|---|---|---|---|
| 1039.642 | 1077.595 | 1130.655 | 1159.716 | 1245.662 | 1301.718 |
| 1328.743 | 1335.786 | 1631.887 | 1659.976 | | |

**88-G6**
**P06748 (NPM_HUMAN) Nucleophosmin**
**[84 0.0011 6/9 22%; 32.6K 4.64]**

| | | | | | |
|---|---|---|---|---|---|
| 910.429 | 931.486 | 974.518 | 1023.514 | 1558.720 | 1568.741 |
| 1582.756 | 1603.767 | 2161.022 | | | |

**Table 2: Proteins recruited to the membrane upon stimulation.**

Peptide mass lists are tabulated below, along with Mascot search summary for each protein spot.

Gel position number: MALDI plate and spot number
SwissProt accession number, SwissProt code, protein name
[MOWSE score, expect value, matching peptides/total peptides, percentage coverage; theoretical MW, pI]
Scores in red indicate a statistically significant identification ($p<0.05$) from Mascot search.

**Plate 75**

Protein stain: silver
Database: SwissProt 47.6 (243668 sequences) – 18 Aug 2005 or
*SwissProt 47.7* (245699 sequences) (human 53508 sequences) – 22 Aug 2005
Taxonomy: unrestricted
Error tolerance: 100 ppm
Variable modifications: CAM-Cys, Met-Ox

Any deviations from these parameters are indicated adjacent to spot number.

**1: 75-A5 (Database: SwissProt 47.7; taxonomy: human; variable modifications: + prop-C)**
**P28331 (NDUS1_HUMAN) NADH-ubiquinone oxidoreductase 75 kDa subunit, mitochondrial precursor**
**[90 6.0e-05 8/9 14%; 79.4K pI 5.89]**

| | | | | | |
|---|---|---|---|---|---|
| 911.329 | 994.144 | 1064.553 | 1225.166 | 1401.754 | 1425.749 |
| 1491.818 | 1607.747 | 1626.756 | 1644.789 | 1839.967 | |

**2: 75-A1 (Taxonomy: human; error tolerance: 75 ppm)**
**P13796 (PLSL_HUMAN) L-plastin**
**[113 2.7e-07 11/18 21%; 70.2K pI 5.20]**

| | | | | | |
|---|---|---|---|---|---|
| 998.552 | 1011.656 | 1051.700 | 1069.638 | 1117.604 | 1135.629 |
| 1338.853 | 1405.827 | 1431.772 | 1518.768 | 1534.836 | 1585.855 |
| 1666.008 | 1675.862 | 1759.870 | 1803.942 | 1831.935 | 1885.038 |

**3: 75-C2 (Database: SwissProt 47.7; taxonomy: human; variable modifications: + prop-C)**
**P30101 (PDIA3_HUMAN) Protein disulfide-isomerase A3 precursor**
**[55 0.74 7/13 11%; 56.7K pI 5.98]**

| | | | | | |
|---|---|---|---|---|---|
| 1172.568 | 1188.557 | 1341.692 | 1359.673 | 1370.713 | 1437.765 |
| 1475.704 | 1515.788 | 1579.879 | 1596.932 | 1782.793 | 1794.813 |
| 2036.004 | | | | | |

**11: 75-A3**
**P30740 (ILEU_HUMAN) Leukocyte elastase inhibitor**
**[161 1.9e-11 15/28 34%; 42.7K pI 5.90]**

| | | | | | |
|---|---|---|---|---|---|
| 1006.510 | 1102.611 | 1126.568 | 1149.597 | 1178.580 | 1179.728 |
| 1194.558 | 1207.651 | 1218.615 | 1230.704 | 1287.705 | 1305.713 |
| 1333.715 | 1346.716 | 1389.778 | 1496.877 | 1510.760 | 1602.784 |
| 1650.800 | 1686.870 | 1785.914 | 1809.803 | 1860.907 | 1896.030 |
| 1934.868 | 1940.931 | 2003.061 | 2035.957 | | |

**16: 75-H3**
**P15428 (PGDH_HUMAN) 15-hydroxyprostaglandin dehydrogenase [NAD+]**
**[68 0.04 6/17 30%; 29.0K pI 5.56]**

| | | | | | |
|---|---|---|---|---|---|
| 1030.601 | 1095.679 | 1212.727 | 1275.642 | 1390.726 | 1421.908 |
| 1512.805 | 1767.829 | 1798.800 | 1809.800 | 1826.800 | 1834.915 |
| 1977.005 | 2008.985 | 2018.972 | 2035.993 | 2044.090 | |

**18: 75-D7 (Database: SwissProt 47.7)**
**P07203 (GPX1_HUMAN) Glutathione peroxidise 1**
**[66 0.068 5/13 28%; 21.9K pI 6.15]**

| | | | | | |
|---|---|---|---|---|---|
| 1154.513 | 1163.596 | 1169.675 | 1313.590 | 1325.779 | 1352.770 |
| 1496.802 | 1496.802 | 1653.958 | 1741.870 | 1758.873 | 1798.797 |
| 2115.034 | | | | | |

**21: 75-H1 (Taxonomy: human; error tolerance: 75 ppm)**
**P61224 (RAP1B_HUMAN) Ras-related protein Rap-1B**
**[76 0.0013 7/25 45%; 20.8K pI 5.65]**

| | | | | | |
|---|---|---|---|---|---|
| 915.459 | 985.634 | 1011.668 | 1018.792 | 1065.719 | 1191.686 |
| 1208.630 | 1220.837 | 1254.771 | 1258.595 | 1314.803 | 1332.756 |
| 1338.816 | 1366.873 | 1424.786 | 1455.760 | 1467.787 | 1494.829 |
| 1554.723 | 1569.725 | 1659.867 | 1665.979 | 1704.003 | 1708.874 |
| 1918.034 | | | | | |

**22: 75-B4**
**Q9H0U4 (RAB1B_HUMAN) Ras-related protein Rab-1B**
**[84 0.00095 6/12 34%; 22.2K pI 5.55]**

| | | | | | |
|---|---|---|---|---|---|
| 990.493 | 1071.628 | 1087.541 | 1102.518 | 1119.542 | 1316.669 |
| 1348.664 | 1377.612 | 1457.729 | 1724.869 | 1798.800 | 2196.205 |

**27: 75-E4**
**P52565 (GDIR1_HUMAN) Rho GDP-dissociation inhibitor 1**
**[77 0.0046 6/9 25%; 23.2K pI 5.02]**

| | | | | | |
|---|---|---|---|---|---|
| 980.488 | 1245.553 | 1261.545 | 1470.745 | 1617.765 | 1751.834 |
| 1773.826 | 1798.795 | 1917.934 | | | |

**31: 75-B8 (Database: SwissProt 47.7; error tolerance 150 ppm)**
**P09104 (ENOG_HUMAN) Gamma-enolase**
**[115 1.7e-07 11/21 30%; 47.1K pI 4.91]**

| | | | | | |
|---|---|---|---|---|---|
| 963.472 | 991.525 | 1014.147 | 1018.774 | 1057.569 | 1088.601 |
| 1100.527 | 1130.622 | 1160.558 | 1235.656 | 1255.622 | 1406.728 |
| 1586.786 | 1599.780 | 1603.774 | 1615.754 | 1617.818 | 1631.757 |
| 1858.952 | 1911.364 | 1970.974 | | | |

**Plate 78 PMF**

Protein stain: Sypro Ruby
Database: SwissProt 47.8 (248831 sequences) – 05 Sep 2005
Taxonomy: Mammals (85577 sequences) or Human (54016 sequences)
Error tolerance: 100 ppm
Variable modifications: CAM-C, Met-ox, prop-C

Any deviations from these parameters are indicated adjacent to spot number.

**8: 78-C6 (Error tolerance: 20 ppm)**
**Q9NVA2 (SEP11_HUMAN) Septin-1**
**[78 0.0014 11/40 26%; 49.2K pI 6.38]**

| | | | | | |
|---|---|---|---|---|---|
| 908.435 | 914.471 | 946.546 | 958.573 | 980.664 | 992.608 |
| 1002.632 | 1035.640 | 1077.576 | 1089.616 | 1123.709 | 1152.556 |
| 1211.766 | 1224.604 | 1233.672 | 1260.879 | 1286.651 | 1332.745 |
| 1361.771 | 1378.675 | 1405.817 | 1433.772 | 1439.780 | 1523.957 |
| 1537.865 | 1555.723 | 1581.937 | 1619.859 | 1641.860 | 1764.900 |
| 1922.902 | 1958.014 | 1962.948 | 1978.997 | 2003.064 | 2035.990 |
| 2070.944 | 2082.993 | 2150.129 | 2193.095 | | |

**10: 78-B4 (Variable modifications: - prop-C)**
**P30740 (ILEU_HUMAN) Leukocyte elastase inhibitor**
**[175 1.7e-13 16/26 37%; 42.7K pI 5.90]**

| | | | | | |
|---|---|---|---|---|---|
| 1003.574 | 1035.601 | 1079.650 | 1102.582 | 1149.571 | 1179.703 |
| 1194.531 | 1027.619 | 1218.596 | 1230.675 | 1240.588 | 1287.678 |
| 1305.689 | 1314.760 | 1327.670 | 1346.704 | 1427.810 | 1496.851 |
| 1510.734 | 1592.721 | 1602.764 | 1634.749 | 1650.791 | 1686.857 |
| 1785.903 | 2052.938 | | | | |

**15: 78-A7 (Error tolerance: 110 ppm)**
**P00491 (PNPH_HUMAN) Purine nucleoside phosphorylase**
**[82 0.00055 9/22 33%; 32.1K pI 6.45]**

| | | | | | |
|---|---|---|---|---|---|
| 968.512 | 1003.570 | 1022.578 | 1188.499 | 1204.494 | 1208.635 |
| 1224.664 | 1229.777 | 1231.762 | 1251.684 | 1417.790 | 1618.840 |
| 1654.795 | 1664.849 | 1741.730 | 1800.933 | 1816.947 | 1874.060 |
| 2009.026 | 2420.293 | 2434.280 | 2508.325 | | |

**17: 78-C7 (Error tolerance: 40 ppm)**
**P62993 (GRB2_HUMAN) Growth factor receptor-bound protein 2**
**[68 0.014 7/24 27%; 25.2K pI 5.89]**

| | | | | | |
|---|---|---|---|---|---|
| 904.363 | 918.481 | 928.480 | 932.454 | 962.520 | 968.503 |
| 986.552 | 1003.591 | 1091.534 | 1212.694 | 1251.682 | 1300.682 |
| 1427.861 | 1506.739 | 1512.693 | 1569.675 | 1618.846 | 1683.848 |
| 1715.914 | 1809.825 | 2003.002 | 2035.990 | 2361.098 | 2420.260 |

**19: 78-A3 (Error tolerance: 25 ppm)**
**P32119 (PRDX2_HUMAN) Peroxiredoxin 2**
**[73 0.0045 7/28 32%; 21.7K pI 5.67]**

| | | | | | |
|---|---|---|---|---|---|
| 905.614 | 924.430 | 964.531 | 972.569 | 978.545 | 1021.582 |
| 1071.682 | 1098.570 | 1111.652 | 1133.626 | 1179.638 | 1194.653 |
| 1211.681 | 1233.668 | 1320.798 | 1388.833 | 1420.852 | 1563.734 |
| 1630.024 | 1683.830 | 1713.791 | 1734.975 | 1756.944 | 1863.072 |
| 1885.058 | 1944.144 | 2035.977 | 2072.258 | | |

**23: 78-E7**
**O00194 (RB27B_HUMAN) Ras-related protein Rab-27B**
**[82 0.00057 9/36 44%; 24.6K pI 5.35]**

| | | | | | |
|---|---|---|---|---|---|
| 942.488 | 964.487 | 1003.575 | 1009.595 | 1023.594 | 1029.582 |
| 1111.606 | 1132.524 | 1151.672 | 1168.630 | 1190.625 | 1212.702 |
| 1244.573 | 1261.697 | 1283.684 | 1361.840 | 1377.790 | 1427.854 |
| 1493.750 | 1533.772 | 1567.769 | 1584.770 | 1600.774 | 1616.772 |
| 1683.829 | 1743.912 | 1790.895 | 1809.834 | 1974.937 | 1996.935 |
| 2036.010 | 2084.017 | 2184.101 | 2367.130 | 2420.253 | 2495.246 |

**29: 78-H7**
**P67936 (PTM4_HUMAN) Tropomyosin alpha 4 chain**
**[81 0.00071 9/27 27%; 28.4K pI 4.67]**

| | | | | | |
|---|---|---|---|---|---|
| 905.590 | 958.535 | 968.475 | 1003.574 | 1030.587 | 1148.554 |
| 1170.662 | 1205.646 | 1243.647 | 1272.636 | 1284.739 | 1298.762 |
| 1332.751 | 1379.824 | 1399.747 | 1446.731 | 1614.771 | 1742.859 |
| 1753.912 | 1923.938 | 1962.948 | 2003.036 | 2036.009 | 2420.267 |
| 2434.285 | 2508.312 | 2629.329 | | | |

**Plate 88 PMF**

Protein stain: SYPRO Ruby
Database: SwissProt 48.6 (259907 sequences) – 16 Dec 2005
Taxonomy: unrestricted
Error tolerance: 50 ppm
Variable modifications: CAM-C, Met-Ox, Prop-C

Any deviations from these parameters are indicated adjacent to spot number.

**4: 88-D1**
**P61157 (ARP3_HUMAN) Actin-like protein 3**
**[76 0.006 7/13 18%; 47.3K 5.61]**

| | | | | | |
|---|---|---|---|---|---|
| 947.507 | 1028.545 | 1057.538 | 1128.587 | 1196.556 | 1214.576 |
| 1243.643 | 1297.666 | 1442.805 | 1448.778 | 1540.773 | 1610.840 |
| 1768.908 | | | | | |

**5: 88-D2**
**P00.352 (AL1A1_HUMAN) Retinal dehydrogenase 1**
**[95 7.8e-05 8/11 21%; 54.7K 6.29]**

| | | | | | |
|---|---|---|---|---|---|
| 939.287 | 1189.655 | 1205.659 | 1221.662 | 1434.772 | 1544.825 |
| 1589.813 | 1645.858 | 1700.811 | 1714.851 | 2005.938 | |

**6: 88-F5**
**P50402 (EMD_HUMAN) Emerin**
**[114 1e-06 9/18 40%; 29.0K 5.26]**

| | | | | | |
|---|---|---|---|---|---|
| 924.438 | 941.493 | 963.481 | 1064.555 | 1085.545 | 1203.665 |
| 1213.616 | 1250.576 | 1255.652 | 1340.653 | 1371.698 | 1379.652 |
| 1396.755 | 1593.781 | 1740.956 | 1922.797 | 1937.942 | 2160.985 |

**20: 88-G4**
**Q15907 (RB11B_HUMAN) Ras-related protein Rab-11B [77 0.0056 7/22 34%; 24.3K 5.65] and**
**P30085 (KCY_HUMAN) UMP-CMP kinase [71 0.02 6/15 35%; 22.2K 5.44] and**
**P32119 (PRDX2_HUMAN) Peroxiredoxin 2 [54 4/9 23%; 21.7K 5.67]**

| | | | | | |
|---|---|---|---|---|---|
| 924.461 | 944.527 | 964.572 | 1021.608 | 1080.611 | 1160.614 |
| 1179.682 | 1211.723 | 1248.637 | 1274.671 | 1289.781 | 1306.659 |
| 1392.708 | 1469.785 | 1479.806 | 1511.779 | 1520.787 | 1563.748 |
| 1585.921 | 1641.829 | 1863.090 | 2386.192 | | |

**25: 88-G5 (Error tolerance: 100 ppm)**
**O00299 (CLIC1_HUMAN) Chloride intracellular channel protein 1**
**[93 0.00014 9/20 37%; 26.8K 5.09]**

| | | | | | |
|---|---|---|---|---|---|
| 957.523 | 963.503 | 987.542 | 1021.543 | 1037.583 | 1065.580 |
| 1078.545 | 1094.553 | 1255.660 | 1281.719 | 1328.690 | 1396.744 |
| 1458.794 | 1472.796 | 1480.745 | 1490.795 | 1572.831 | 1588.882 |
| 1601.858 | 1844.982 | | | | |

**30: 88-H6 (variable modifications: + prop-C)**
**P13489 (RINI_HUMAN) Ribonuclease inhibitor**
**[60 0.28 6/10 17%; 49.8K 4.71]**

| | | | | | |
|---|---|---|---|---|---|
| 963.455 | 1209.675 | 1255.599 | 1323.594 | 1397.558 | 1513.739 |
| 1530.723 | 1612.756 | 1630.772 | 2202.889 | | |

**Table 5: Proteins lost from the soluble fraction upon stimulation.**

Peptide mass lists are tabulated below, along with Mascot search summary for each protein spot.

MALDI plate and spot number
SwissProt accession number, SwissProt code, protein name
[MOWSE score, expect value, matching peptides/total peptides, percentage coverage; theoretical MW, pI]
Scores in red indicate a statistically significant identification ($p<0.05$).

**Plate 83**

Gel stain: SYPRO Ruby protein stain
Database: SwissProt 48.2 (259907 sequences) – 16 Dec 2005
Taxonomy: unrestricted
Error tolerance: 100 ppm
Variable modifications: CAM-C, Met-ox, Prop-C

**83-G1**
**P06733 (ENOA_HUMAN) Alpha-enolase**
**[96 5.6e-05 7/8 22%; 47.0K 6.99]**

| | | | | | |
|---|---|---|---|---|---|
| 1143.692 | 1406.743 | 1425.769 | 1541.833 | 1556.839 | 1633.894 |
| 1713.916 | 1805.023 | | | | |

**83-A3**
**P02794 (FRIH_HUMAN) Ferritin heavy chain**
**[67 0.049 5/11 25%; 21.1K 5.30]**

| | | | | | |
|---|---|---|---|---|---|
| 1098.597 | 1135.662 | 1148.618 | 1153.656 | 1281.701 | 1294.700 |
| 1303.610 | 1345.634 | 1452.704 | 1643.805 | 1816.844 | |

**83-D4**
**P07339 (CATD_HUMAN) Cathepsin D precursor**
**[105 1.7e-06 11/20 31%; 44.5K 6.10]**

| | | | | | |
|---|---|---|---|---|---|
| 963.466 | 1065.617 | 1160.670 | 1191.713 | 1196.723 | 1239.673 |
| 1255.678 | 1271.637 | 1312.710 | 1405.756 | 1421.768 | 1437.742 |
| 1462.678 | 1601.828 | 1617.804 | 1803.836 | 1858.909 | 1975.022 |
| 2004.992 | 2350.060 | | | | |

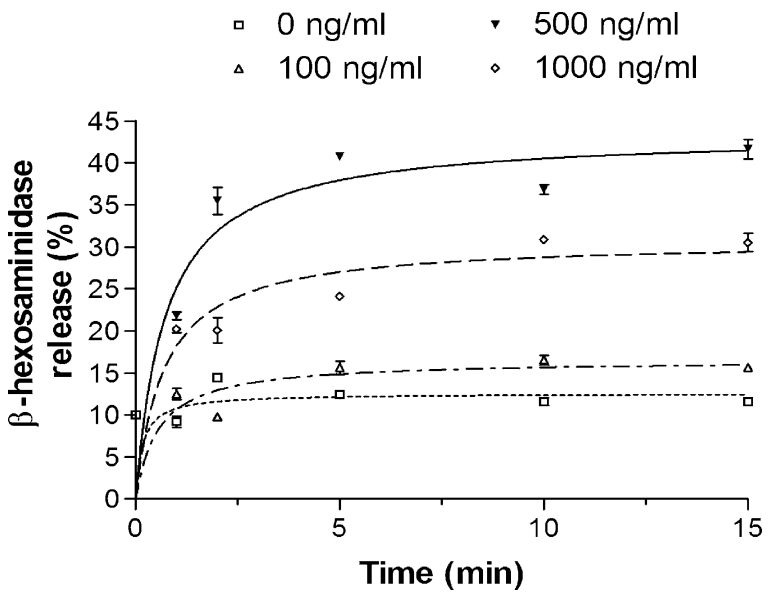
0 ng/ml
500 ng/ml
100 ng/ml
1000 ng/ml
β-hexosaminidase release (%)
45
40
35
30
25
20
15
10
5
0
0
5
10
15
Time (min)

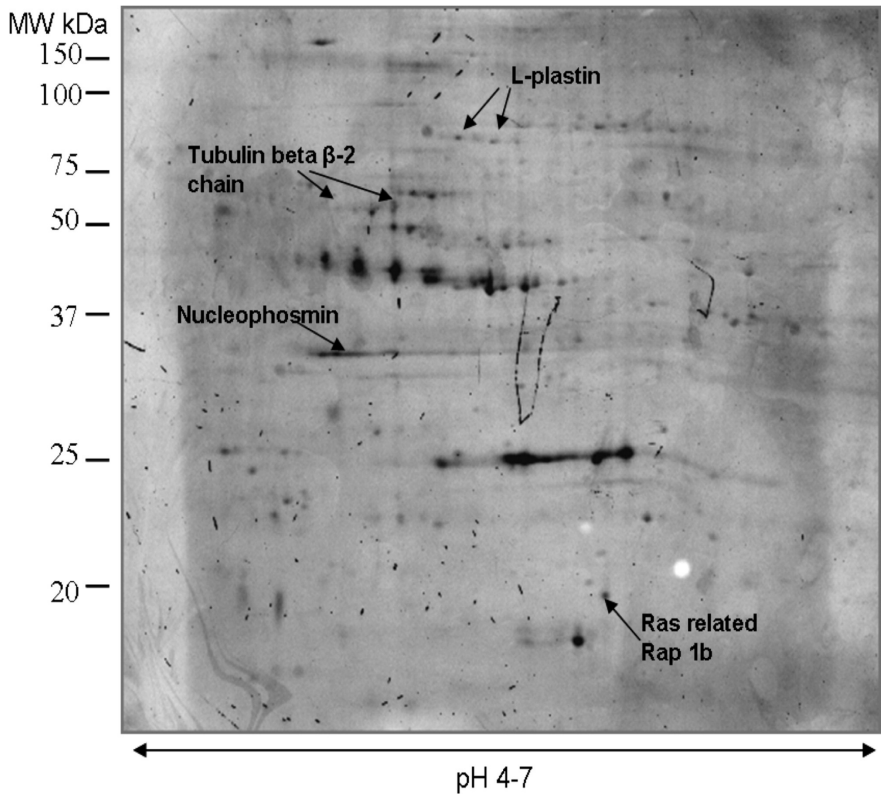
MW kDa
150
100
75
50
37
25
20
L-plastin
Tubulin beta β-2 chain
Nucleophosmin
Ras related Rap 1b
pH 4-7

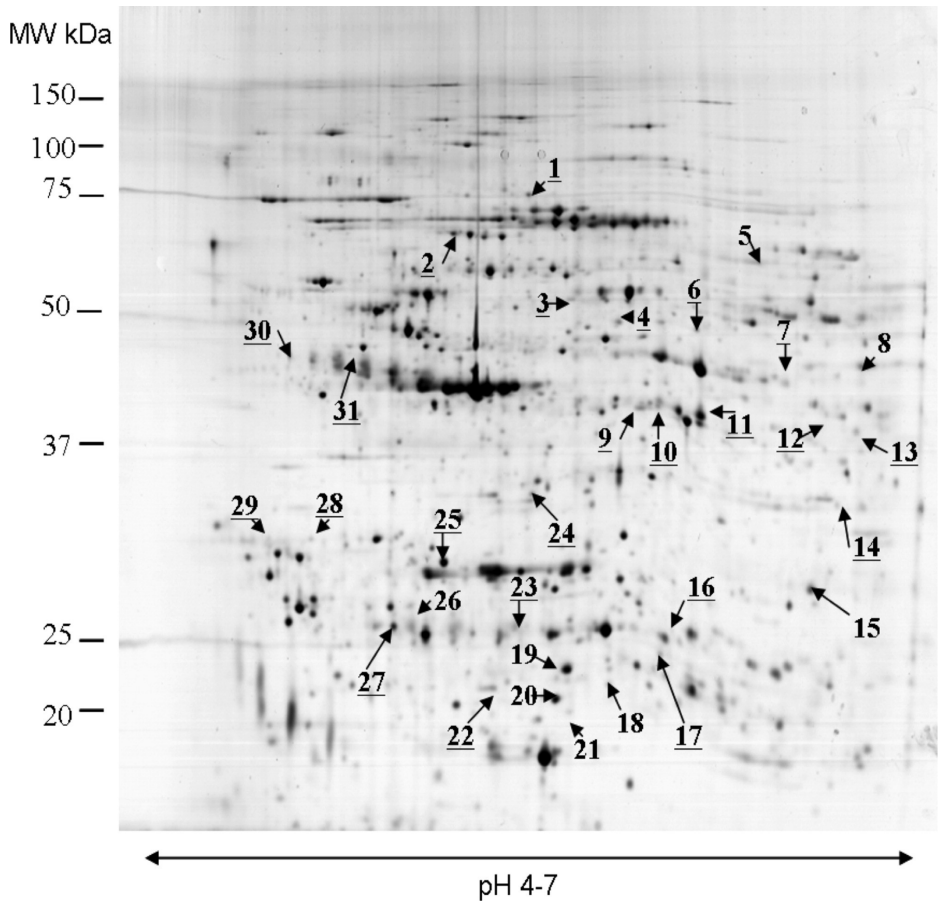
MW kDa
150
100
75
50
37
25
20
1
2
3
4
5
6
7
8
9
10
11
12
13
14
15
16
17
18
19
20
21
22
23
24
25
26
27
28
29
30
31
pH 4-7

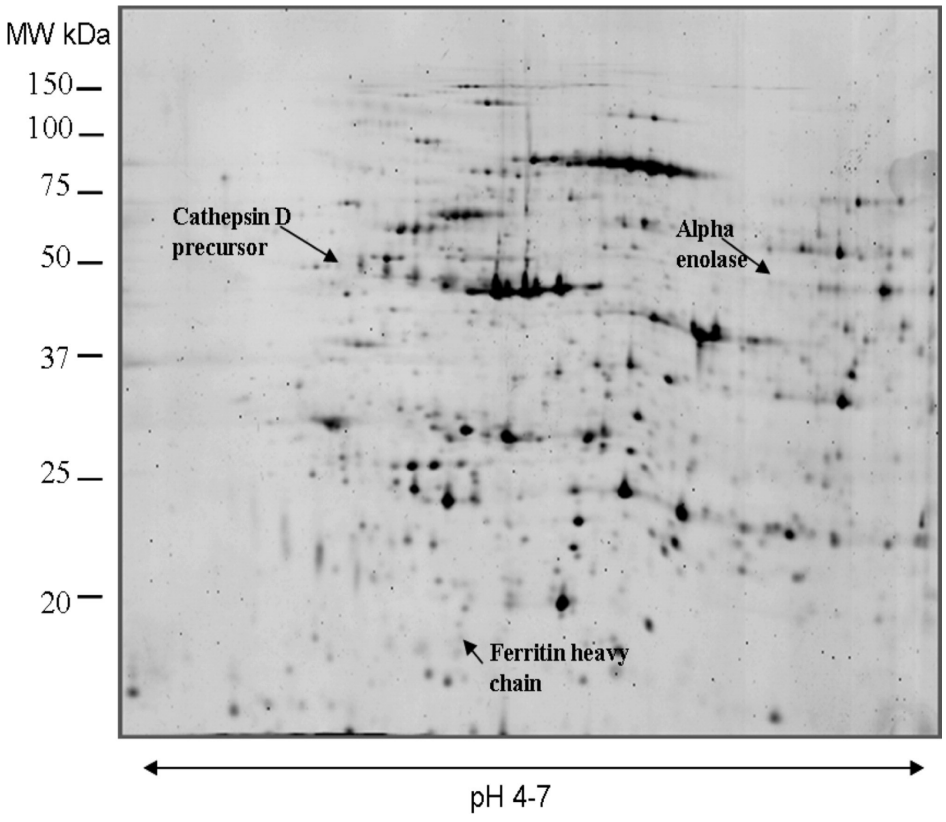
MW kDa
150
100
75
50
37
25
20
Cathepsin D precursor
Alpha enolase
Ferritin heavy chain
pH 4-7

LAD2 secretion

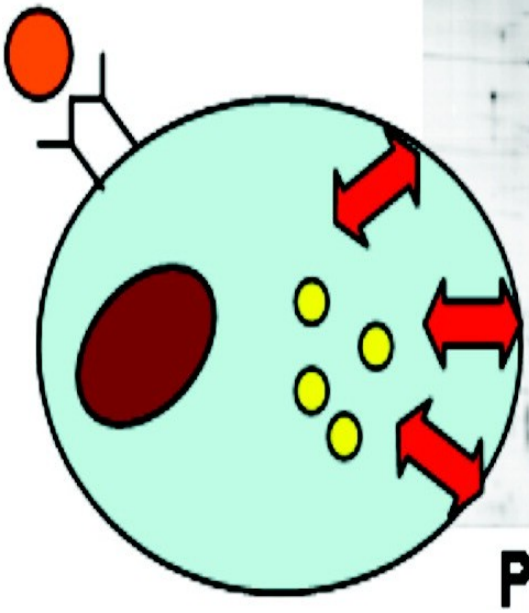

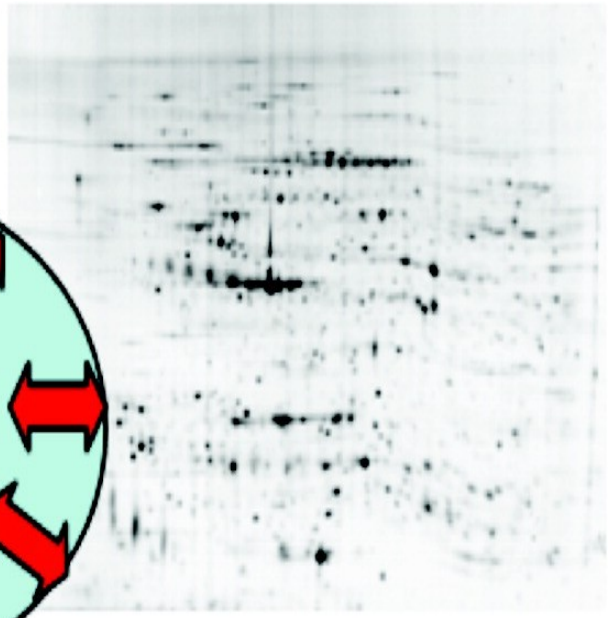

Protein relocation